ABSTRACT

Title of Document: AN ENTROPIC THEORY OF DAMAGE WITH APPLICATIONS TO CORROSION-FATIGUE STRUCTURAL INTEGRITY ASSESSMENT

Anahita Imanian, PhD, 2015

Directed By: Professor Mohammad Modarres

Department of Mechanical Engineering

This dissertation demonstrates an explanation of damage and reliability of critical components and structures within the second law of thermodynamics. The approach relies on the fundamentals of irreversible thermodynamics, specifically the concept of entropy generation due to materials degradation as an index of damage. All failure mechanisms that cause degradation, damage accumulation and ultimate failure share a common feature, namely *energy dissipation*. Energy dissipation, as a fundamental measure for irreversibility in a thermodynamic treatment of non-equilibrium processes, leads to and can be expressed in terms of

entropy generation. The dissertation proposes a theory of damage by relating entropy generation to energy dissipation via generalized thermodynamic forces and thermodynamic fluxes that formally describes the resulting damage.

Following the proposed theory of entropic damage, an approach to reliability and integrity characterization based on thermodynamic entropy is discussed. It is shown that the variability in the amount of the thermodynamic-based damage and uncertainties about the parameters of a distribution model describing the variability, leads to a more consistent and broader definition of the well know time-to-failure distribution in reliability engineering. As such it has been shown that the reliability function can be derived from the thermodynamic laws rather than estimated from the observed failure histories. Furthermore, using the superior advantages of the use of entropy generation and accumulation as a damage index in comparison to common observable markers of damage such as crack size, a method is proposed to explain the prognostics and health management (PHM) in terms of the entropic damage.

The proposed entropic-based damage theory to reliability and integrity is then demonstrated through experimental validation. Using this theorem, the corrosion-fatigue entropy generation function is derived, evaluated and employed for structural integrity, reliability assessment and remaining useful life (RUL) prediction of Aluminum 7075-T651 specimens tested.

AN ENTROPIC THEORY OF DAMAGE WITH APPLICATIONS TO CORROSION-FATIGUE STRUCTURAL INTEGRITY ASSESSMENT

By

Anahita Imanian

Dissertation submitted to the Faculty of the Graduate School of the

University of Maryland, College Park, in partial fulfillment

of the requirements for the degree of

Doctorate of Philosophy

2015

Advisory Committee:

Professor Mohammad Modarres, Chair/Advisor
Professor Mohammad Al-Sheikhly, Dean's Representative
Professor Hugh Alan Bruck
Professor Abhijit Dasgupta
Associate Professor Enrique Lopez Droguett

Dedication

this dissertation is greatly dedicated to my beloved mother and father,

Mahin Mahmoodkhani and Enayatollah Imanian

My beloved husband

Amir

whose sacrificial care for me and my child,

made it possible for me to complete this work

And to my little brilliant girl

Rojina

Acknowledgment

I would like to express my special appreciation and thanks to my advisor Professor Mohammad Modarres, he has been an incredible mentor for me. I would like to thank him for encouraging my research and for allowing me to grow as a research scientist. His advice on both research as well as on my career have been priceless. I appreciate all his contributions of time, brilliant comments and suggestions, and funding to make my Ph.D. experience productive and stimulating.

I would like to thank my other dissertation committee members who also showed a great support and interest in my work. Thanks to Professor Abhijit Dasgupta and Associate Professor Enrique Lopez Droguett. I am very grateful to Professor Hugh Alan Bruck for his support; he provided the DIC instrument that helped me greatly in experimental measurement. Also, thanks to Professor Mohamad Al-Sheikhly and Professor Chunsheng Wang for support and willingness to set time aside to answer my questions.

My genuine and heartfelt thanks go to Professor Aaron Barkatt who supported me by providing some lab equipment over almost two years. My sincere thanks go to Mr. Mohammad Nuhi who supported and inspired me throughout this journey. He is a great experimentalist and has taught me a lot about instrumentation. I would also like to thank Dr. Mehdi Amiri for his help while he was a postdoctoral student in Professor Modarres' group at the Risk and Reliability Center, University of Maryland.

A special thanks to my family. I would like to express my sincere appreciation to my beloved husband Amir who has encouraged and supported me academically and emotionally through the rough road to finish this dissertation. My special thanks to my

loving daughter Rojina. Her birth in the middle of this path was like a beginning of all things, hopes and dream for possibilities.

Words cannot express how thankful I am to my mother, my father, my sister Elina and my brother Mahyar for all of the sacrifices that they've made on my behalf. Your prayers for me were what sustained me through this endeavor. I would also like to thank my student colleagues Victor Ontiveros, Abdallah Altamimi, Chonlagarn Iamsumang, Elaheh Rabiei, Azadeh Keshtgar and all my friends at the University of Maryland, College Park who incented me to strive towards my goal.

Table of Contents

List of Tables

List of Figures

List of symbols

Parameter	Unit	Description
A_D	m^2	Damage surface area
A_n	m^2	Initial (pre-damage) cross section area
A_i	J	Chemical affinity (i =1, 2, ...)
$\tilde{A}_M$	v	Electrochemical affinity of oxidation reaction
$\tilde{A}_O$	v	Electrochemical affinity of reduction reaction
a_{i_n}	Unitless	Degradation trend parameter at cycle n
$b(D_f)$	Unitless	Endurance threshold distribution
D	Unitless	Damage
d	Unitless	Superscript for dissipative part of the entropy
D_f	Unitless	Damage threshold
d^eS	($J\ K^{-1}$)	Variation of exchange entropy
d^dS	($J\ K^{-1}$)	Variation of dissipative entropy
E	v	Applied over-potential
E_{corr}	v	Electrode open circuit potential
$E_{M_{act,a}}$	v	Anodic over-potential for oxidation reaction
$E_{M_{act,c}}$	v	Cathodic over-potential for oxidation reaction
$E_{O_{act,a}}$	v	Anodic over-potential for reduction reaction

$E_{O_{act,c}}$	v	Cathodic over-potential for reduction reaction
$E_{M_{conc,c}}$	v	Concentration over-potential for cathodic oxidation
$E_{O_{conc,c}}$	v	Concentration over-potential for cathodic reduction
e	Unitless	Superscript for exchange part of the entropy
F	C mol^{-1}	Faraday's constant
$f(D)$	Unitless	Damage probability distribution function
$g(t)$	Unitless	Time to failure probability distribution function
$h(D)$	Unitless	PDF of the damage prediction at l^{th} step ahead
I	A	Electrical current
I_{Sh}	Unitless	Shannon's missing information function
K_B		Boltzmann constant
J_s	J K^{-1} m^{-2} s^{-1}	Total entropy flow per unit area per unit time
J_q	W m^{-2}	Heat flux
J_k	mol m^{-2} s^{-1}	Diffusion flux
$J_{M,a}$	A	Irreversible flux of anodic half-reaction of oxidation
$J_{M,c}$	A	Irreversible flux of cathodic half-reaction of oxidation
$J_{O,a}$	A	Irreversible flux of anodic half-reaction of reduction
$J_{O,c}$	A	Irreversible flux of cathodic half-reaction of reduction
n	Cycle	Number of fatigue load cycles

N_s	Unitless	Number of set of random samples drawn from a probability distribution function
P	Pa	Maximum stress
P_r	Unitless	Probability
R	Unitless	Reliability function
RUL	Cycle	RUL cumulative probability distribution
S	J K^{-1}	Entropy
s	J Kg^{-1} K^{-1}	Specific entropy
T	K	Temperature
T_c	Cycle	Endurance level
T_r	s	Time random variable
t_c	s	Failure time
V	m^3	Volume element
V_m	m^3 mol^{-1}	Molar volume
v_i	mol s^{-1}	Chemical reaction rate
W	Unitless	Number of possible microstates
w	Unitless	Importance weight
$\boldsymbol{x}_n$	Unitless	The degradation trend parameter vector at cycle *n*
z_M	Unitless	Number of moles of electrons exchanged in the oxidation process

z_O	Unitless	Number of moles of electrons exchanged in the oxidation process
α_M	Unitless	Charge transport coefficient for the oxidation process
α_O	Unitless	Charge transport coefficient for the reduction process
β	Vary	Standard deviation for noise normal distribution
γ	J m^{-3} K^{-1}	Volumetric entropy
γ_d	J m^{-3} K^{-1}	Cumulative volumetric entropy generation
γ_{d_E}	J m^{-3} K^{-1}	Entropic-endurance
ϵ_p	Unitless	Plastic strain
λ	Cycle	Distribution parameter
μ_k	J mol^{-1}	Chemical potential
$\tilde{\mu}_k$	J mol^{-1}	Electrochemical potential
ρ	Kg m^{-3}	Density
σ	J m^{-3} K^{-1}	Entropy generation per unit volume per unit time
σ_{act}	J m^{-3} K^{-1}	Entropy generation due to activation losses per unit volume per unit time
σ_{conc}	J m^{-3} K^{-1}	Entropy generation due to concentration losses per unit volume per unit time
σ_Ω	J m^{-3} K^{-1}	Entropy generation due to Ohmic losses per unit volume per unit time
τ	Pa	Stress tensor

τ_m	Pa	Hydrostatic part of the stress
ν	Unitless	Stoichiometric coefficient
ψ	v	Potential of the external field
θ	Unitless	Entropic damage measurement noise
ω_{a_i}	Unitless	Degradation trend parameter noise PDF

List of Acronyms

CE	Counter electrode
CTF	Cycle to failure
CTIT	Classic theory of irreversible thermodynamic
DEG	Degradation-entropy generation
EDTF	Entropic damage to failure
FL	Fault level
FMMEA	Failure modes, mechanisms, and effects analysis
kNN	k-nearest neighborhood
MEPP	Maximum entropy production principle
PHM	Prognostics and health management
PDF	Probability density function
PF	Particle filter
RE	Reference electrode
RUL	Remaining useful life
TTF	Time to failure
WE	Working electrode

1. Chapter 1: Introduction

1.1 Motivation

Cumulative hazard and cumulative damage models are important for reliability and structural integrity assessment. In fact, there is a substantial gap between available reliability and integrity techniques and the fundamental science of materials degradation dynamics needed to model early failure prediction and assessment of the remaining useful life (RUL) of critical components and structures. To advance the traditional structural integrity and life estimation approaches, this research proposes an alternative science-based approach to damage assessment and reliability modeling based on the second law of thermodynamics.

This research proposes and demonstrates that the entropy generated by multiple failure mechanism processes, which lead to materials degradation, can be used as a more representative and integrated index of damage. The proposed entropic-based damage index offers a unified and more comprehensive measure of damage. It is known that energy dissipations associated with failure mechanisms, which lead to materials degradation, involve irreversible processes resulting in entropy generation which is physically measurable as the materials degrade. It is, therefore, hypothesized, and later demonstrated, that entropy generation is a suitable measure of damage as it allows for more accurate estimation of reliability of components, integrity of structures and the expended and remaining life of materials.

One application of the proposed concept is the entropic characterization of corrosion-fatigue degradation mechanism. As will be discussed later, this approach, i.e. the entropy-based damage approach, is used to assess the degradation and reliability of aluminum 7075-T651 specimens. Furthermore, a standard entropy-based damage prognostic and health management (PHM) approach is employed in integrity assessment and remaining useful life prediction of aluminum 7075-T651 specimens. Using entropy as a thermodynamic state function for damage characterization, this research discusses the effectiveness of entropic-endurance threshold for probabilistic prognostic purposes.

1.2 Research Objectives and Approach

In this research, an answer is sought to the question of how the entropy generation of failure mechanisms can describe the amount of materials damage and how such description is used to characterize reliability and integrity of components and structures. Using a theorem relating entropy generation to dissipative processes via generalized thermodynamic forces and thermodynamic fluxes, this dissertation develops a model that formally describes the damage parameter. Having developed the proposed entropic damage model over time, the entropy-based reliability and PHM models are derived. To demonstrate the proposed approach, this dissertation elaborates on one synergistic degradation process and failure mechanism: corrosion-fatigue.

In considering the use of entropy for corrosion-fatigue structural integrity assessment, this research involves the following steps: In considering the use of entropy for corrosion-fatigue structural integrity assessment, this research involves the following steps:

- Provides a mathematical formalism for entropy generation as a damage index, derived in terms of multiple dissipative processes occurring in corrosion-fatigue.
- Explores the hypothesis that degradation-caused entropy generation is independent of the cumulative damage path, i.e., the generated entropy is constant for all units as they reach an undesired level of damage.
- Demonstrates the advantages of such an entropic damage that uses entropy generation as an index.
- Uses the proposed entropic damage for assessing reliability of components and structures and demonstrates the approach on Al 7075-T651 alloy specimens tested for corrosion-fatigue damage.
- Assesses the performance of the entropy-based PHM framework for prediction of Al 7075-T651 alloy specimen RULs. Other features of entropy such as its capability in studying the synergistic effects arising from interaction of synergistic corrosion and fatigue processes [1, 2] are also investigated within experimental records.

In order to meet these objectives, the process employed in research can be summarized as shown in the following flowchart:

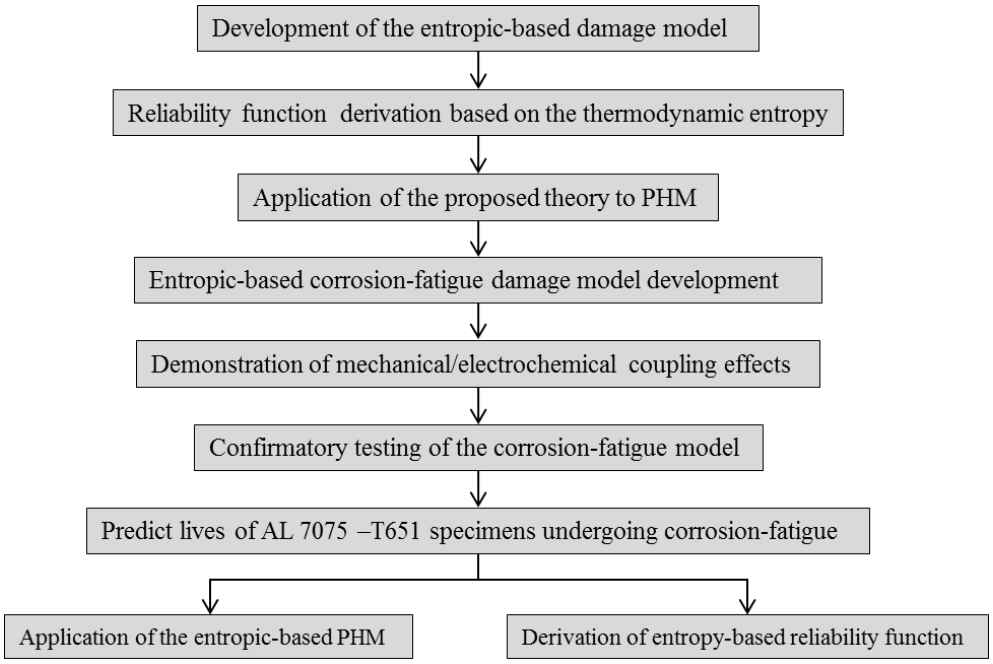

Figure 1.1. Dissertation processes flowchart

1.3 Contributions

The main contributions in this dissertation are:

- Development and confirmation of an entropic theory of damage based on the second law of thermodynamics along with an entropic index that quantifies the amount of linear cumulative damage or cumulative hazard.
- Characterization and derivation of reliability functions such as the time-to-failure probability density function within the second law of thermodynamics. This includes providing definition for the notions of entropic damage to failure (EDTF) and entropic-endurance.

- Description of the entropic-based structural reliability properties such as expended life and RUL.
- Demonstration of the superior advantages in using the entropic damage index in PHM applications.
- Development of a corrosion-fatigue thermodynamics model that is used in the subsequent experimental verifications as an example of a complex interactive degradation phenomenon.
- Demonstration of the applications of the proposed theorem and approaches in corrosion-fatigue degradation mechanism, simulated in the laboratory environment. The thermodynamic entropy generated "as a measure of damage" in the corrosion-fatigue degradation mechanism was evaluated in terms of associated dissipative processes for Al 7075-T65.
- Introduction of a more consistent definition of reliability of items in the context of the entropic-damage along with its demonstration to the corrosion-fatigue degradation of the specimens tested.
- Applications of the entropic-damage in reliability assessment, in PHM and RUL estimation of specimens tested have been demonstrated.

1.4 Outline of the Dissertation

The remainder of the dissertation is organized as follows. Chapter 2 provides a review of the background and related studies. In Chapter 3, the thermodynamics

background necessary for the assessment of entropic damage is presented. In Chapter 4, I discuss the uncertainties related to the damage evolution model, the ability of entropy to provide the best life model, and the entropy-based reliability and PHM approaches are demonstrated. Chapter 5 derives a function of entropy generation resulting from corrosion-fatigue degradation mechanism through identification of associated dissipative processes. Chapter 6 illustrates the materials and the experimental procedure employed for simulation of corrosion-fatigue degradation mechanism and investigates the mechano-chemical synergistic effect. In chapter 7, the entropy-based damage model is employed to evaluate the degradation evolution trend of Al 7075-T651 specimens subjected to corrosion-fatigue; the entropy based reliability method is applied to obtain the reliability of specimens at a particular time; and the RUL of specimens are estimated via the entropy-based PHM framework. Chapter 8 concludes and provides recommendations for future work.

2. Chapter 2: Background and Review of Major Related Works

This chapter provides an overview of the key literature on degradation and damage models used in the assessment of reliability of systems and integrity of structures. It mainly concentrates on the notion of entropy generation as a measure of degradation and damage in materials, and reviews the state-of-the-art advances in entropic treatment of damage followed by a discussion on the generalization of the entropic concept to damage characterization. Specific examples of thermodynamic-based treatments of damage are presented and degradation mechanisms such as fatigue, wear and corrosion, including coupled (interacting) mechanisms, are discussed. The superior advantages of an entropic approach in reliability assessment and RUL predictions of structures and components are discussed and compared with the current methods and approaches.

2.1 Failure Models

Reliability engineering has evolved significantly over the past few decades in the way it addresses risk and reliability challenges in design, manufacturing and operation. The evolution of reliability modeling began with the traditional generic handbook-based reliability prediction methods such as those advocated in MIL-HDBK-217F [3], Telcordia SR-332 [4], and FIDES [5] relied on the analysis of field data (with complex and varied operating and environmental conditions), with the assumption that the

failure rates are constant. However, numerous studies have shown that by not considering unit-to-unit minor variations and differences in the field operation of units (especially in identical units), the generic and even more unit-specific data led to misleading and inaccurate reliability assessments [6, 7].

More recently, formal consideration of empirically based physics and mechanistic models in reliability analysis, herein referred to as the physics of failure (PoF) approach, has been a significant improvement over the conventional historical data and reliability test approaches [8, 9, 10, 11, 12]. The PoF approach simulates empirically based physical models of failure based on the science of failure mechanisms such as fatigue, fracture, wear, and corrosion.

There are three possible PoF modeling frameworks subject to the nature of the underlying failure and degradation mechanism: the stress-strength model, the performance-requirement model, and the damage-endurance model [13]. The most common PoF model of failure is the damage-endurance model, where degradation in the form of irreversible cumulative damage occurs. The stress aggregate drives the cumulative damage metric. Cumulative damage may not degrade performance; however, the item fails when the cumulative damage exceeds its endurance limit. In all these models, damage is an abstract notion. Traditionally, to measure damage, observable surrogates or markers of damage, such as crack length [1] or amount of wear [14] have been used to characterize damage. Next section elaborates on damage definition concept and its effect on degradation and structural integrity assessment.

2.2 Damage Parameter Definitions

The common definition of damage relies on the field variables chosen to describe the anticipated aging or degradation process which is subjective and dependent on the choices of the observable variables in the underlying physical processes leading to damage. For example, for fatigue, damage variables used to describe the expected damage include the ratio of instantaneous to final crack lengths [15], the linear summation of normalized number of cycles accumulated at different stresses (Miner's rule) [16], the accumulation of normalized surface layer stress [17], the cumulative plastic strain ratio [18], the linear summation of persistent slip band length ratio [19], the accumulation of the endurance limit ratio [20, 21] and the ratio of defect surface area to total cross section area [22]. For wear damage, the local plastic deformation [23], the wear volume [14] and delamination of composites [24] have been used. Moreover, the definition of damage can vary at different geometric scales. For example, in the corrosion-fatigue degradation mechanism, transmission electron microscopy and dislocation modeling studies show that at the nano-scale, adsorbed hydrogen ions localize plastic deformation and lower the energy required for fracture, resulting in degradation [25]. At the micro-scale level, it has been shown that weakness of oxide film for extensive plastic deformation relative to the underlying metal may result in the localization of slip bands and a reduction in near-surface plasticity, ultimately leading to the formation of dislocation structures and voids [26]. At the meso-scale level, damage constitutes the growth and coalescence of micro cracks that initiate a crack. At

a macro-scale level, damage is defined as the growth and propagation of macro-cracks that result in a final fracture [1].

2.3 Thermodynamic Characterizations of Damage

It is evident that the true damage in nearly all degradation processes is larger than the observed markers of damage. For example, in fatigue involving plastic deformation, many unobserved subsurface micro cracks, among other types of damage are present before a marker of damage such as a large enough crack becomes observable. Difficulties in proposing a consistent definition of damage from the physical and mechanical points of view have compelled some researchers to look for a microscopically consistent definition in the context of the continuum damage mechanics (CDM) [22, 1]. For example, in CDM, damage, D, as a thermodynamic internal variable is defined as the effective surface density of microdefects:

$$D = \frac{A_D}{A_i} \tag{1}$$

where A_D is the damage surface area and A_i is the initial (pre-damage) cross section area. Due to the difficulty of directly measuring the density of defects on the surface or volume of materials, Lemaitre [22] used the strain equivalent principle to correlate between other measurable properties of material (e.g. variation of elastic strain, module of elasticity, micro-hardness, density, and plastic strain) and damage. However, these different damage indices do not provide a consistent measure of damage that covers both observable and unobservable damages. In a thermodynamic framework, Lemaitre [22] also utilized the thermodynamic relation between damage rate and dissipation of

energy to derive the constitutive equations. He provides a comprehensive discussion on the general methods of deriving the constitutive equations for different degradation processes. However, the analytical expression of the dissipation potential (or equivalently damage rate potential) is not of concern in this study. Rather, we propose a general way to quantify damage that is applicable to different degradation phenomena. Therefore, a more objective, consistent and broad definition of damage is necessary and plausible. To attain this goal, this study elaborates on the concept of material damage within the thermodynamic framework.

Thermodynamically, all failure mechanisms (degradation processes) leading to damage share a common characteristic, which is the dissipation of energy. In thermodynamics, dissipation of energy is the basic measure of irreversibility, which is the main feature of the degradation processes in materials [27]. Chemical reactions, release of heat, diffusion of materials, plastic deformation, and other means of energy production involve dissipative processes. In turn, dissipation of energy can be quantified by the *entropy generation* within the context of the irreversible thermodynamics. Therefore, dissipation (or equivalently entropy generation) can be considered as a substitute for characterization of damage. This forms the basis of a theory pursued in this study, in which entropy generation is considered as a broad index of damage and thus offers a science-based alternative to model a wide range of damage processes and describes a more fundamental science of reliability and integrity assessment. Dissipative processes can be directly related to thermodynamic entropy, for example plasticity and

dislocations [28, 29], erosion-corrosion [30], wear and fracture, fretting-corrosion [31], thermal degradation [32], and associated failure of tribological components [33, 34].

2.3.1 Entropy for damage characterization from statistical mechanics approach

There are two distinct interpretations of entropy for damage characterization. In the statistical mechanics microscopic interpretation of entropy introduced by Boltzman [35], the connection between damage and entropy may be established by using Equation 2 where the entropy, S, "as a macroscopic thermodynamic quantity can be connected with the statistical microscopic quantity" [36] , W, describing "the probability that the system will exist in the state it is, relative to all the possible states it could be in" [37].

$$S = K_B \ln W \tag{2}$$

where $K_B = 1.38 \times 10^{-23}$JK^{-1} is the Boltzmann constant. Using this approach, Basaran et al. [37, 38, 39, 40] and Temfack and Basaran [41] introduced a damage variable model as the ratio of probability of a microstructure state, W, to the original reference state probability, W_0. They calculated entropy generation and employed the Boltzmann notion of statistical entropy to describe the damage growth function for Pb/Sn solder alloys. Tucker et al. [42] and Chan et al. [43] also utilized the statistical

mechanics [44] interpretation of entropy for modeling damage and fatigue fracture initiations and growth in solder joints. In their model, damage is defined as the cumulative distribution function corresponding to the probability of a microstructure state, W, occurring as a function of an entropic measure.

2.3.2 Use of second law of thermodynamics approach for damage characterization

The macroscopic interpretation of entropy as the second law of thermodynamics offers an alternative definition of damage based on the interesting aspect of the principle of entropy increase. According to the second law of thermodynamics, natural processes evolve spontaneously in one direction only through the increase of entropy [45]. In accordance with the principle of entropy increase, manufactured organized components return to their natural conditions through degradation, which reduces the integrity of material properties to the point where the components are no longer functional [27].

Feinberg and Widom [46, 47] made early efforts to describe a thermodynamic-based definition of damage. They developed a thermodynamic characterization of degradation dynamics, which employs the Gibbs free energy as a measure of material or component parameter degradation. According to their model, disorder/damage must increase entropy or reduce thermodynamic energies. The use of Gibbs free energy and its reduction to represent the degradation, however, is only valid when the pressure and temperature of the system remain constant [2], which constrained their model of

degradation to isothermal-isobaric conditions (e.g., Gibbs energy-based damage modeling cannot capture degradations due to thermal losses). Furthermore, they assumed that change in the system characteristic results from a log-time aging behavior versus time. This is true only if the damage accumulates at a fixed rate, which assumes constant use and accumulation of damage at a constant rate [27]. In fact, the emerging field of damage mechanics tracks entropy and thermodynamic energies to quantify the behavior of irreversible degradations, including tribological processes such as friction and wear [48, 49, 50, 51, 34] and fretting and fatigue [52, 53, 54, 37], that incline to increase entropy generation of the components or structures. In what follows we elaborate on the concept of entropy employed to represent some irreversible processes including fatigue, wear and stress corrosion cracking.

2.3.2.1 Use of entropy in modeling fatigue damage

Particularly in the fatigue and fracture community, thermodynamic treatment of damage has been broadly studied. Early efforts at entropy-based modeling date back to the studies of Whaley et al. [55, 56, 54]. They suggested that the entropy generation during fatigue is associated with the plastic energy dissipation, and can be assessed by the cumulative amount of plastic energy per unit temperature of material. Furthermore, they suggested that at the beginning of fatigue failure, the total entropy gain due to irreversible plastic deformation is constant. Ital'yantsev [57, 58], likewise, showed that fatigue failure occurs when the material gains a critical value of cumulative entropy. He proposed mathematical conditions for failure and showed that the entropy of a

material tends to increase until failure occurs, after which the entropy generation vanishes. However, Whaley et al. and Ital'yantsev offered no experimental observations or quantification of entropy accumulation to support their claim.

Basaran et al. [37, 38, 39, 40] , Tucker et al. [42] and Chan et al. [43] used the concept of entropy from statistical mechanics [44] for modeling damage and fatigue fracture initiation and growth in solder joints. Their model uses a small-strains small-displacements assumption with application to electronic packaging under isothermal conditions. Furthermore, it does not make a clear distinction between the total entropy and the entropy generation.

Naderi et al. [59] demonstrate the potential of employing the concept of thermodynamic entropy generation to assess degradation in processes involving metal fatigue. They report a broad series of experiments performed to determine the fatigue fracture entropy for two different metals. In particular, they show that the maximum value of cumulative entropy for Aluminum 6061-T6 undergoing low-cycle fatigue is about 4 MJ/m^3 K and about 60 MJ/m^3 K for stainless steel 304L, irrespective of the load amplitude, geometry, size of specimen, frequency, and stress state. Similarly, Amiri et al. [60] show that the accumulated entropy generation for bending low-cycle fatigue tests of Aluminum 6061-T6 samples is nearly constant, with the average of 4.07 MJ/m^3K, regardless of the displacement amplitude. They show that empirical fatigue models such as Miner's rule, Coffin-Manson Equation, and Paris law can be deduced from thermodynamic consideration.

Ontiveros [52] also employed entropy generation to estimate time to fatigue crack initiation in notched specimens subjected to uniaxial cyclic load in high-cycle regimes. Results of their work suggest that the time for short fatigue crack can be estimated via cumulative entropy generation.

2.3.2.2 Use of entropy in wear damage treatment

Thermodynamic treatment of wear damage has also been extensively studied. Early attempts date back to the work of Klamecki [49], who performed a near-equilibrium analysis via entropy generation to demonstrate energy dissipation in friction processes. Klamecki showed that entropy could be used to describe all dissipative processes in sliding contact, including wear damage. The experimental work of Doelling et al. [50] showed that the amount of mass removal due to wear has a linear correlation with entropy flow. Entropy flow was calculated by means of a calorimeter via measuring heat generation and temperature rise at contact surfaces. They also showed that the classical Archard's wear law [14] is a consequence of the second law of thermodynamics and can be derived in terms of a functional relationship between wear and entropy flow. It is to be noted that the work of Doelling et al. pertained to steady-state conditions where entropy flow is equal to entropy generation. Doelling et al. argued that it is the entropy generation that represents exhaustion (i.e., degradation) of a thermodynamic system and showed that experimental measurement of the entropy flow is simpler than entropy generation that merely requires measuring entropy due to heat and mass exchange with the environment. Several other studies are available on

thermodynamic assessment and, specifically, entropic assessment of tribosystems [61, 62, 63]. Amiri and Khonsari (2010) provide a comprehensive review of the entropic approach to friction and wear problems.

2.3.2.3 Use of entropy in degradation analysis of structural material behavior under mechanical load and corrosion

The strain response of electrode potential or work function has long been of interest in relation to a wide range of problems, including corrosion in structural materials under load [64, 65, 66, 29], coupling of electronic properties to stress in semiconductor devices [67, 68], diffusion [69, 70], and metallurgy [71]. For metals under corrosion and mechanical loads, Gutman [29] identified the influence of elastic and plastic deformation on anodic dissolution rates and vice versa (i.e., the mechano-chemical effect). He formulated the entropy generation as the sum of entropy generation due to electrochemical reactions and plastic deformations, and correlated the associated thermodynamic fluxes and forces by phenomenological equations [72]. In the thermodynamic analysis given by [73, 30, 74, 66], the contribution of elastic deformation, plastic deformation and hydrogen dissolved on the anodic corrosion current density is discussed for corroding metal specimens under hydrogen charged stressed conditions. Other researchers [75, 76, 77, 65] have studied the effect of elastic strain on the change in metal reactivity to the varying working function. For example, Smertanin [77] demonstrated that at equilibrium, Maxwell's thermodynamic relationship is valid between the derivative of the surface stress of the electrode, with

respect to its superficial charge density, and the derivative of electrode potential to tangential strain variable. Although all these studies use the thermodynamic laws to interpret the electro-mechano-chemical effects between mechanical deformation and active corrosion dissolution rate, none of them utilizes the concept of entropy as an index of damage resulting from the associated dissipative processes.

The preceding literatures review demonstrates that the concept of entropy provides a science-based modeling approach to a wide range of damage processes with promising results in fatigue and fracture mechanics, and tribology processes [59]. Following this trend, Bryant et al. [78] established a more general relationship between the damage of systems undergoing irreversible dissipative processes and the associated entropy generation called the Degradation-Entropy Generation (DEG) theorem. In their approach Bryant et al., linked the traditional damage measure based on the observable markers of damage (e.g. wear volume, crack size and corrosion mass loss) to the associated entropy generation through a linear relation. Their actual results focused on tribological systems with a single dissipative process of wear [78]. They concluded that the famous Archard law [14] for measuring wear in fretting wear is the consequence of the DEG theorem. Clearly, connection of the entropy generation to markers of damage requires that the entropy generated exclusively be generated for the specific degradation process that caused the observable marker. While this is theoretically valid, measurement of the entropy that can be exclusively attributed to a marker of damage would be nearly impossible.

Using a theorem relating entropy generation to the dissipation processes via the generalized thermodynamic forces and thermodynamic fluxes, this study offers an alternative science-based damage assessment approach to formally describe the resulting damage. This entropy-based damage modeling approach is demonstrated by modeling the corrosion-fatigue degradation and failure mechanism. Using the entropy-based damage approach allows analysts to develop the corresponding structural integrity, reliability function, and assess the RUL of such structures. This recognition also let us to introduce an entropy-based PHM framework which provides a strong foundation for failure prediction and RUL assessment of critical components and structures.

2.4 Life Prediction Models

Prognostic and health management approaches provide information about the performance and RUL of components by modeling degradation propagation. The techniques included in the PHM provide warnings before failures happen, reduce life cycle cost of inspection, and improve qualification tests assisted in design and manufacturing. Generally speaking, PHM models [79, 80] are developed to combine the knowledge of the past deterioration trend and the current degradation state with the endurance threshold to estimate the RUL [81] . Traditionally, these methods rely on the condition of the performance data which are evaluated by empirically based PoF models [8, 9, 11, 12] or data-driven techniques such as machine learning algorithms

[82, 83, 84]. The PoF models utilize the specific knowledge of products, such as failure mechanisms, material properties, loading profile and geometry [8, 9, 11, 12, 10]. However, such empirical methods are limited to simple failure mechanisms and are hard to model when multiple competing and common cause failure mechanisms are involved. In general, data-driven approaches such as neural networks [82], decision tree classifiers [83] and Bayesian techniques [85, 86] can be considered as a black box operation that can obtain the complex relationship and degradation trend in the data without the need for the particular product characteristics such as the degradation mechanism or material properties. The weakness of data-driven techniques is that they cannot differentiate different failure modes and mechanisms in the system [87]. "This limits root-cause analysis, and increases uncertainty in validation and verification" [87]. In data-driven approaches, RUL is typically assessed by estimating damage trend, performing an appropriate extrapolation to the damage trend, and calculating RUL from the intersection of the extrapolated damage to a defined endurance threshold. In these methods, the threshold, such as the mean value of endurance threshold, or a conservative lower-bound of endurance threshold, is commonly selected deterministically. However, the specification of the endurance threshold has a critical effect on the RUL prediction performance [88]. For example, setting a high threshold value can cause a component to fail before its scheduled time. On the other hand, a conservative low threshold value can result in the premature abandonment of the component from the operation.

Using entropy generation as an index of damage can remedy some of the shortcomings of PoF and data driven approaches in several ways. In comparison with PoF models which traditionally rely on the dominant failure mechanism, entropy generation provides a consistent and far broader interpretation and measure of damage by incorporating multiple competing and common cause degradation mechanisms. By its nature, entropy "as a measure of uncertainty" [43, 89, 40] comprises the variabilities in the microstructure states. Therefore, it can provide the better estimate of life in the absence of detailed microstructural observations [43]. Furthermore, the entropy-based PHM framework suggested in this study enables to tackle the issue of endurance threshold determination by taking the advantage of entropy being as a thermodynamic state function independent of the path of the failure (which commonly depends on factors such as geometry, load and frequency of load) from the initial state to the final failed state of the material, considering a known endurance limit [59, 27].

2.5 Corrosion-Fatigue Degradation Models

The assessment of the corrosion-fatigue degradation mechanism as an example of the proposed entropic-based reliability and integrity assessment is of technical and economic interest, as it can severely jeopardize the structural integrity and safety of critical structures such as off-shore structures, naval vessels, and naval airframes [90, 91, 92]. Common practices for corrosion-fatigue structural integrity assessment in metals and alloys have isolated and evaluated the damage characteristics at different

life stages. As such, the corrosion-fatigue damage process is divided into four stages: 1) the pit nucleation, 2) growth of the nucleated pit, 3) surface crack initiation and its growth into a through crack phase, and 4) through-crack growth to a prescribed critical length. For each of these stages, researchers have proposed empirical models for the life estimation [93, 94, 95, 96, 97, 98, 99, 12]. In these models, the pit growth rate is typically follows the Kondo model [93], whereby the pit remains hemispherical in shape and grows at a constant volumetric rate. The Linear Elastic Fracture Mechanism (LEFM) and Elasto-Plastic Fracture Mechanism (EPFM) are often applied at the crack propagation stage and final instability [100, 11, 91]. The lifetime of a component subject to corrosion-fatigue is estimated by the sum of the lifetime obtained from empirical models developed for each stage. In this study, using a theorem relating entropy generation to dissipative phenomena, the corrosion-fatigue entropy generation function was derived, evaluated and employed to assess the degradation evolution of Al7075-T651 specimens.

3. Chapter 3: An Entropic Theory of Damage

3.1 Entropy Generation and Damage

It was stated earlier that damage resulting from the degradation processes could be viewed as the consequence of dissipation of energies (refer to Figure 3.1) that can be more generally expressed by entropy as its index such that:

$$\text{Damage} \equiv \text{Entropy}$$

Figure 3.1. Entropy generation relationship to damage

An immediate question that arises is how to characterize the deterioration of integrity due to the resulting damage in terms of the entropy generation. Consistent with the second law of thermodynamics, entropy does not obey the conservation law. Processes occurring inside the system may be reversible or irreversible. Reversible processes inside a system may lead to transfer of entropy resulting from heat and material exchange from one part of the system to other parts of the interior, but these processes do not generate entropy. Irreversible processes inside a system, however, do generate entropy, and hence this factor must be taken into account in computing the level of entropy.

3.2 Fundamentals of Irreversible Thermodynamics

For a system with properties being continuous functions of space and time, irreversible processes can be described by formulating the first and second laws of thermodynamics. If the system involves chemical reaction and work of any forms, Gibbs [101] shows that the change in internal energy, U, of the system on the basis of combining the first and second laws of thermodynamics would be:

$$\dot{U} = T\dot{S} + \dot{W} + \sum_{i=1}^{m} X_i J_i + \sum_{k=1}^{r} \mu_k v_k \quad (3)$$

where S is the entropy of the system, T is temperature, W is the mechanical work due to deformation in the bulk of the system, X_i is generalized thermodynamic force (such as pressure), J_i is the generalized thermodynamic flux (such as volume rate), μ_k is the chemical potential and $v_k$is the chemical reaction rate of the k^{th} component.

Note that $\dot{W}$ in Equation 3, is associated with the work of quasi-conservative forces and $X_i J_i$ is associated with the work of dissipative forces. According to Ziggler [102], forces applied on the system can be divided into quasi-conservative and dissipative forces. Quasi-conservative forces can be derived from free energy and do not contribute to dissipations [27].

According to the principles of thermodynamics for any macroscopic system, the variation of the entropy, S, of the system can be written as the sum of two terms [103, 2, 45]:

$$dS = d^e S + d^d S \tag{4}$$

where superscripts e and d represent the exchange and dissipative parts of the entropy, respectively. The term $d^e S$ is the entropy supplied to the system by surrounding elements through transfer of mass and heat (e.g., in an open system where wear and corrosion mechanisms occur), which may be positive or negative. The term $d^d S$ is the entropy produced inside of the system where according to the second law of thermodynamics must be zero for reversible transformations and positive ($d^d \mathrm{S} \geq 0$) for irreversible transformations of the system with increase of disorder.

In order to calculate the entropy generation in terms of experimentally measurable quantities, Equation 4 can be written in a local form that is appropriate for description of systems where the densities of extensive properties such as mass and energy are continues functions of space coordinates [103]. As such, S can be defined for a domain g by the means of specific entropy s per unit mass (described by density ρ and volume V) as $S = \int_g \rho s dV$, and the rate of exchanged entropy can be obtained as:

$$\frac{d^e S}{dt} = -\int^{\Omega} \boldsymbol{J}_s . \boldsymbol{n}_s dA \tag{5}$$

where $\boldsymbol{J}_s$ is a vector of the total entropy flow per unit area per unit time (flux), crossing the boundary between the system and its surroundings, and $\boldsymbol{n}_s$ is a normal vector. Moreover, the rate of $d^d S$ can be obtained from:

$$\frac{d^d S}{dt} = \int^V \sigma dV \tag{6}$$

where σ is the entropy generation per unit volume per unit time. Figure 3.2 illustrates the concept of entropy generation and entropy flow in a system.

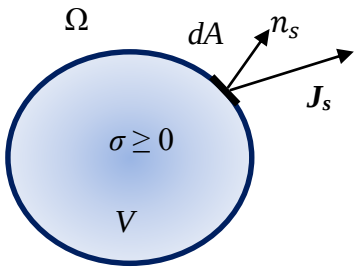

Figure 3.2. Entropy generation and entropy flow for a system

Using Equation 4, 5, 6 and Gauss' theorem [45, 103], the entropy balance, Equation (6), can be expressed in local form as:

$$\rho \frac{ds}{dt} + \nabla . \boldsymbol{J}_s = \sigma \tag{7}$$

According to the second law of thermodynamics, the entropy generation per unit volume per unit time within the system, σ, must be zero for reversible transformations and positive for irreversible transformations of the system with increase of disorder. This suggests the use of entropy as a measure of disorder or damage ("the larger the

disorder, the larger the entropy" [104]), that characterizes expenditure of the system's life. Accordingly, the damage rate of the system is closely connected to entropy generation, which accumulates progressively over time and degrades the system until its final breakdown [48, 27].

In order to assess damage induced in the system, every fundamental dissipative process active in the system should be identified. Using the conservation (balance laws) of energy, mass and momentum, along with the Gibbs relation shown in Equation 3 [101] and under the hypothesis of local equilibrium, the balance equation for entropy can be derived in terms of explicit expressions as in Equation 8 [2, 103]. The concept of local equilibrium simply assumes that for a thermodynamic system, intensive variables such as internal energy, u, molar number per unit volume, n_k, and specific volume, v, that define entropy per unit mass $s(u, \mathrm{v}, n_k)$ and necessarily define the macroscopic state of the system can also be well defined locally [103]. According to the local equilibrium hypothesis, it is assumed that although the total system is not in equilibrium, over a small region, there exist a state of local equilibrium where the local entropy, s, is the same function, ($s = s(u, \mathrm{v}, n_k)$), of u, v and n_k, and, specifically, Equation 3 remains valid.

$$\frac{d\gamma}{dt} = -\nabla.\left(\frac{\boldsymbol{J}_q - \sum_{k=1}^{n}(c_m\psi + \mu_k)\boldsymbol{J}_k}{T}\right) \tag{8}$$

$$+\frac{1}{T^2}\boldsymbol{J}_q.\nabla T-\Sigma_{k=1}^{n}\boldsymbol{J_k}\left(\nabla\frac{\mu_k}{T}\right)+\frac{1}{T}\boldsymbol{\tau}\colon\dot{\boldsymbol{\epsilon}}_p+\frac{1}{T}\Sigma_{j=1}^{r}v_j\,A_j$$
$$+\frac{1}{T}\Sigma_{m=1}^{h}c_m\boldsymbol{J}_m(-\nabla\psi)$$

where $\gamma=\rho s$ is volumetric entropy, $\boldsymbol{J}_q$ is heat flux, $\boldsymbol{J}_k$ is diffusion flow, $\boldsymbol{J}_m$ represents fluxes resulting from external fields (magnetic and electrical) such as electrical current, $A_j=-\Sigma_{i=1}^{u}\mu_i\nu_{ji}$ is chemical affinity or chemical reaction potential difference, $\boldsymbol{\tau}$ is the stress tensor, $\dot{\boldsymbol{\epsilon}}_p$ is plastic strain rate tensor, ψ is potential of the external field such as electrical potential difference, and c_m is the coupling constant. External forces may result from different factors including electrical fields, magnetic fields and gravity fields where the corresponding fluxes are electrical currents, magnetic currents and velocity. For example, in the case of an electric field, $E=-\nabla\psi$ is the electric potential, $\boldsymbol{I}=\Sigma_{m=1}^{h}c_m\boldsymbol{J}_m$, is current density and $c_m=Fz_m$, where F is the Faraday constant and z_m is the number of moles of electrons. Each term in Equation 7 is derived from the various mechanisms involved, which define the macroscopic state of the complete system. By comparing Equation 8 with Equation 7 we can state:

$$\boldsymbol{J}_s=\frac{\boldsymbol{J}_q-\sum_{k=1}^{n}(c_m\psi+\mu_k)\boldsymbol{J}_k}{T} \tag{9}$$

$$\sigma=\frac{1}{T^2}\boldsymbol{J}_q.\nabla T-\Sigma_{k=1}^{n}\boldsymbol{J}_k\left(\nabla\frac{\mu_k}{T}\right)+\frac{1}{T}\boldsymbol{\tau}\colon\dot{\boldsymbol{\epsilon}}_p+\frac{1}{T}\Sigma_{j=1}^{r}v_j\,A_j$$
$$+\frac{1}{T}\Sigma_{m=1}^{h}c_m\boldsymbol{J}_m(-\nabla\psi) \tag{10}$$

where Equation 9 shows the entropy flux resulting from heat exchange and material exchange, and the presence of an external field. Equation 10 represents the total energy

dissipation terms from the system that (from left to the right) include heat conduction energy, diffusion energy, mechanical energy, chemical energy, and external field energy (such as magnetic, electrical, radiation and gravity). Equation 10 is fundamental to non-equilibrium thermodynamics, and represents the entropy generation σ as the bilinear form of thermodynamic forces and fluxes as:

$$\sigma = \Sigma_{i=1}^{m} X_i J_i \tag{11}$$

It is through this form that the contributions from the applicable thermodynamic forces and fluxes are expressed. A major task in developing an entropic damage framework is to properly identify applicable dissipative processes, the appropriate set of fluxes, and the conjugate driving forces. For example, Table 3.1 lists some of the thermodynamic forces and fluxes for some of the irreversible processes including fatigue, corrosion, creep, wear and irradiation.

Table 3.1. Corresponding forces and fluxes for select dissipative processes [27]

Primary mechanism	**Thermodynamic force, *X***	**Thermodynamic flow, *J***	**Examples**
Heat conduction	Temperature gradient, $\nabla(1/T)$	Heat flux, q	Fatigue, creep, wear
Plastic deformation of solids	Stress, τ/T	Plastic strain, $\dot{\epsilon}_p$	Fatigue, creep, wear
Chemical reaction	Reaction affinity, A_k/T	Reaction rate, ν_k	Corrosion, wear
Mass diffusion	Chemical potential, $-\nabla(\frac{\mu_k}{T})$	Diffusion flux, j_k	Wear, creep
Electrochemical reaction	Electrochemical potential, $\tilde{A}/T$	Corrosion current density, i_{corr}	Corrosion

Irradiation	Particle flux density, A_r/T	Velocity of target atoms after collision, $\dot{v}_r$	Irradiation damage
Annihilation of lattice sites	Creep driving force,$(\tau - \omega_1)/T$	Creep deformation rate, R	Creep

3.3 Local Equilibrium Hypothesis for Non-equilibrium Thermodynamics

To better understand the thermodynamics of materials damage, let us briefly elaborate on some fundamental thermodynamics concepts. First, we must notice that all degradation mechanisms leading to damage are in non-equilibrium states [45]. Therefore, equilibrium thermodynamics —which is merely concerned with equilibrium in which a system attains maximum entropy with zero entropy generation rate, $\sigma = 0$ —cannot describe the degradation. The classic theory of irreversible thermodynamic (CTIT), on the other hand, enables us to cope with non-equilibrium changes from place to place and over time. The most important hypothesis underlying CTIT is undoubtedly the local equilibrium hypothesis. According to Lebon et al. [45], the local equilibrium hypothesis states that the local and instantaneous relations between a system's properties are the same as for a uniform system in equilibrium. Lebon et al. also suggest that, mentally, systems can be divided into cells that are sufficiently large for microscopic fluctuations to be negligible but sufficiently small so that equilibrium can be realized in each individual cell to a good approximation. Based on the local equilibrium hypothesis, each cell is assumed to be in equilibrium state. Thermodynamic properties are uniform within each individual cell, but can differ among neighboring

cells. Also, in each individual cell the equilibrium state can change with time [45]. Furthermore, two timescales are suggested to check the applicability of the local equilibrium assumption. The first timescale, t_m, is the time elapsed for an individual cell to attain equilibrium, and it is of the order of the time interval between two successive collisions between particles, i.e., 10^{-12} s, at normal pressure and temperature. The second timescale, t_M, is related to the time required for macroscopic change of the system. This may be the time required for macroscopic damage induced in the system, or may be related to the duration of an experiment. The ratio of these two timescales is called the Deborah number (i.e., $De = t_m/t_M$). For $De \ll 1$, the local equilibrium hypothesis is applicable where relevant variables evolve on a large timescale t_M and practically do not change over the time t_m. However, the hypothesis is not appropriate for describing situations for which large values of De are typical for fast or high frequency phenomena such as ultrasound propagation, shock waves and nuclear collisions, or when other variables, not found at equilibrium, are able to influence the process. This is, for instance, the case for polymers found in long molecular chains where their configuration affects their activities substantially. Other examples include super-fluids and superconductors whose irregular properties require introduction of extra variables [45]. The corrosion-fatigue degradation process used in this study as an example is considered a relatively slow phenomenon occurring over a long period and therefore justifying use of the local equilibrium hypothesis.

3.4 Outline of the Proposed Entropic Theory of Damage

Qualification of the local equilibrium hypothesis for slow degradation mechanisms enables the use of Equation 10 and allows us to express the evolutionary trend of the total volumetric generated entropy, γ_d, representing damage, D, by:

$$D \sim \gamma_d|t = \int_0^t [\sigma|X_i(u), \boldsymbol{J}_i(u)]du \tag{12}$$

where $\gamma_d|t$ is the monotonically increasing cumulative entropy starting at time zero from a theoretical value of zero or practically some initial entropy, γ_{d_0}, to an entropic-endurance value, γ_{d_E}, that makes the component functionally non-performing. Examples of the entropic-endurance level include a point where it is judged that a small margin to failure might remain. The following attributes describe key properties of the entropic-endurance level:

1. Entropic-endurance describes the capacity of a unit to withstand entropy.
2. Entropic-endurance of the same units is equal.
3. Entropic-endurance of different units is different.
4. Entropic-endurance can be measured and involves stochastic variability.

This research proposes an entropic theory of damage in which the normalized thermodynamic entropy generation, due to all degradation processes that act individually or synergistically, is considered as the index of the resulting damage.

Accordingly, I define damage due to all degradation processes by the general damage index:

$$D = \frac{\gamma_d - \gamma_{d_0}}{\gamma_{d_E} - \gamma_{d_0}} \tag{13}$$

When cumulative total entropy γ_d reaches this entropic-endurance, γ_{d_E}, from initial damage entropy, γ_{d_0}, it may be assumed that, for all practical purposes, the component or structure is considered as failed. At this level, the corresponding damage index reaches unity whereby cumulative damage reaches a level beyond which the specimen or component reaches a zone of concern (but not necessarily the point of failure that might be interpreted as an observable damage). When the level of entropic-based cumulative damage is normalized to represent the damage, care must be taken not to correspond it to an observable damage marker. For example, if a specimen underwent fatigue degradation resulting in fracture, this end effect (i.e., failure point) does not necessarily represent the time when the normalized entropic-damage reaches unity. In an entropic-based damage the entropic-endurance level should be selected as the point when the damage is deemed intolerable and high enough that occurrence of a failure is imminent. Selection of appropriate entropic-endurance can be made from reliability and integrity testing or from engineering judgment.

In this study, the evaluation of damage is quantified relative to the initial damage value of zero. The initial entropic-damage can be calculated using the correlation between the rate of damage and damage at different stage of degradation [1].

At its core, the entropic-based definition of damage is consistent with the widely used PoF models (i.e. stress-strength, performance requirement and damage-endurance models [13]) discussed above. The underlying process of failure in all three models is consistent with the entropic theory of damage discussed earlier, as entropy is generated in all of them and they all involve energy dissipation. For example, in the stress-strength model, the assumption is that the unit (e.g., a structure, system or component) fails if the stress (mechanical, thermal, electrical or radiation) exceeds the strength (e.g., yielding point, tear resistance, melting point, burst resistance, and conductive heat resistance). In the context of the entropic definition of damage, the stress-strength failure involves rapid and nearly instantaneous generation of entropy that exceeds the corresponding entropic limit that describes failure. Similarly, according to the thermodynamic practice of damage-endurance model, as discussed earlier, gradual degradation involving energy dissipation leads to the cumulative entropic damage, and the item fails only when the cumulative entropic damage exceeds the entropic endurance. In the performance-requirement model, the assumption is that the unit's performance characteristic is satisfactory if it falls within an acceptable tolerance limit. Consistent with the entropic definition of damage, the underlying processes that cause performance decline (e.g., an increase in resistivity of resistors, loss of efficiency of rotating machinery, and declining luminosity) also involve energy dissipation along with entropy generation over time. In this case, accumulation of entropy itself can represent the unit's performance decline until a requirement such as safety margin or minimum output requirement (considered as the entropic endurance) is violated.

4. Chapter 4: An Entropy-Based Reliability and PHM Approaches

Since energy dissipation leads to entropy generation, the total entropy generated in any degradation process can be established through the measurement of dissipated energies, and which can then be used as an index of damage. Such index is used to derive the time of failure of structures and components. This description, therefore, connects the second law of thermodynamics to the conventional models of reliability engineering used in life assessment. Accordingly, this chapter provides a formalism to relate the entropy-based damage to the corresponding reliability models of life. In comparison with the conventional probabilistic reliability quantities, deriving the reliability function in terms of entropy generation can offer a fundamental approach to representation of reliability. Finally, this chapter, provides an entropy-based PHM framework to estimate the RUL of critical components and structures, and discusses the superior features of the proposed entropic damage index as compared to the common observable markers of damage.

4.1 Entropy as a Measure of Uncertainty

Uncertainties associated with models used to measure degradation and damage in materials are due to natural variabilities in the microstructure states (e.g., chemical composition phases, point and planar defects, grain orientations, grain boundaries,

dislocations and configurations of microcracks and cavities). These microstructure features must be incorporated into damage models through experimental observation, which is difficult to accomplish in practice. These challenges have inspired some researchers to use entropy as "a measure of uncertainty" for prediction and assessment of damage [1, 41, 37, 39]. In terms of uncertainty, entropy is linked with the missing information about which of the microstates with energy *E* is occupied at any instant (i.e. the probability, W, that the system will exist in the state with energy *E*, relative to all the possible states). Boltzmann relates entropy to the probabilistic microscopic behavior of matter as a measure of uncertainty, or more specifically, missing information, by his well-known expression shown in Equation 2. Jaynes [105] also described uncertainty of microstates in statistical mechanics [44] through information theory (using Shannon's notion of information entropy as a measure of information uncertainty [106]) and the maximum entropy production principle (MEPP) [105], where, given incomplete information about possible states in which a system could exist, the preferred state is the one that maximizes the entropy. In accordance with his study, supposing a set of W possible microstates with probabilities P_{r_i} as the probability for microstate i, where $i = 1, 2, \dots, W$, Leff [89] also shows that one can acquire the least biased estimate of the individual probabilities. This is done by obtaining the set of probabilities that maximizes Shannon's missing information function [106] as:

$$I_{Sh} = -c \sum_{i=1}^{W} P_{r_i} \ln P_{r_i} \tag{14}$$

relative to known constraints, where c = constant. If the only constraint remains that the sum of the probabilities is equal to one, the probability of microstates can be obtained as: $P_{r_i} = 1/W$ for all i, and $I_{Sh} = c \ln W$. If the arbitrary constant c is selected to be K_B, Boltzmann's constant, the Shannon missing information function I becomes identical to the Boltzmann entropy, $S = K_B \ln W$. Therefore, S can be inferred as the extent of missing information—that is uncertainty [89].

4.2 Reliability Assessment Based on Entropic Damage

Material, environmental, operational and other variabilities in degradation processes and other events leading to damage impose uncertainties on the damage trends (i.e., normalized total entropy growth as the index), D, and resulting time to failure (TTF) points as depicted in Figure 4.1. However, since entropy comprises the uncertainties resulting from microstate variabilities (i.e., the major source of aleatory uncertainties), the entropic damage to failure (EDTF) data points should result in the thinner distribution compared with TTF distribution. At the ideal condition, in the absence of epistemic and aleatory uncertainties, the trends of thermodynamic entropy "as a state function" should converge to merely a deterministic EDTF.

When the preceding sources of uncertainty are introduced, the variations in the resulting entropies can be described by a random variable and described as the probability density function (PDF) of the EDTF data points. This PDF can then be used

to describe the life expended and the useful remaining life of the component or structure.

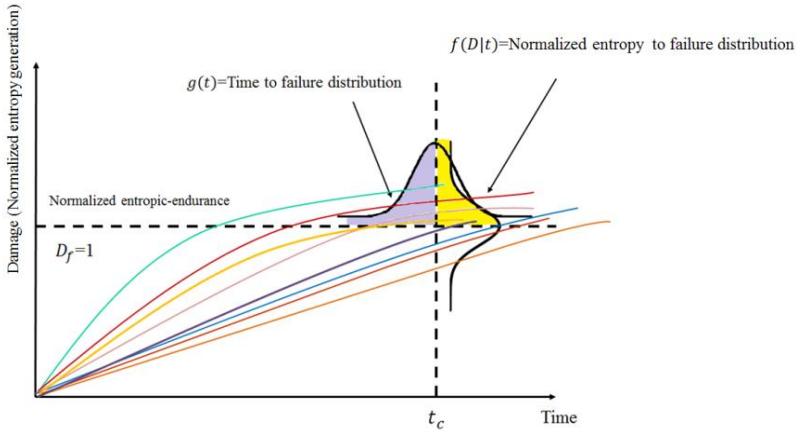

Figure 4.1. Distribution of damage to failure data points and time to failure data points

Mathematically, the probability that the random variable, D, (i.e., the cumulative damage at the observed failure time, t_c) exceeds D_f (the normalized "entropic-endurance" discussed earlier) is equal to the probability that the random variable T (time to failure) is less than t_c. Accordingly, one can derive the time to failure PDF, $g(t)$, from the thermodynamic index of damage (i.e., cumulative entropy) described by the PDF, $f(D)$:

$$P_r(T \leq t_c) = \int_0^{t_c} g(t)dt = 1 - \int_0^{D_f=1} f(D)dD \quad (15)$$

By deriving the time to failure PDF, we can find the pertinent reliability function at particular time t_c which is expressed by Equation 16. In this formulation, the reliability

function is derived based on the total thermodynamic entropy generated, rather than estimated, from historical TTF data.

$$R(t_c) = 1 - P_r(T \leq t_c) = \int_0^{D_f=1} f(D)dD \quad (16)$$

Using thermodynamics entropy to obtain the reliability function reveals the contribution of underlying failure mechanisms (e.g., fatigue, corrosion and heat losses) to the overall failure, while capturing the interactions among them. Therefore, in comparison with conventional reliability assessment based on historical data, deriving the reliability function in terms of EDTF PDF provides a theoretical and systematic approach for the health management of degraded components where the degradation process contributions in generating the entropy are recognized.

Developing conventional reliability function, however, as discussed earlier can result in inefficient inspection, repair and replacement schedule and cost, unplanned component and structure shut down, and safety impacts (e.g. possible exposure of hazardous parts to personnel and environment). The deployment of PHM methods can provide safety, operational and functional benefits along with reducing the epistemic uncertainties associated with data (e.g. updating the prior data with new evidence using well-known methods such as Bayesian updating, Kalman filtering, constraint optimization and particle filter).

4.3 Entropy-Based Damage PHM Framework

In this study we propose an entropy-based PHM framework to estimate the RUL of critical components and structures. This framework shown in Figure 4.2, benefits from conventional data driven techniques and the superior advantages of the use of entropy as a damage index in comparison with common observable markers of damage.

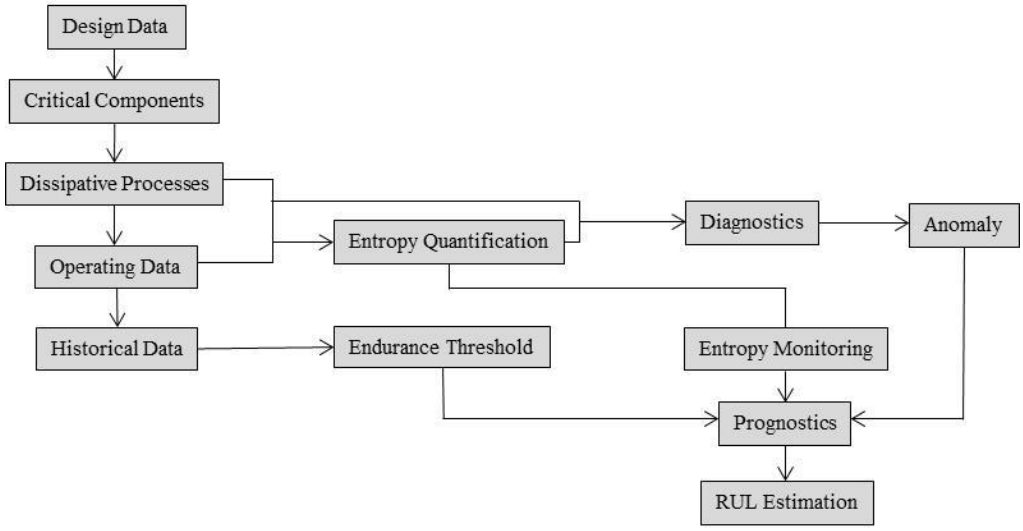

Figure 4.2. Entropy-based damage PHM framework

According to this framework, the health assessment and RUL prediction can be implemented in four steps. First, the dissipative processes and associated data in the critical components under aging are determined. These processes and relevant parameters can be identified by the traditional Failure Modes, Mechanisms, and Effects Analysis (FMMEA), which identifies the potential failure mechanisms for products under certain environmental and operating conditions. The volumetric entropy as a

parameter of damage, which includes all the interactive failure mechanisms, is quantified then. The second step is the extraction of the features (e.g., root mean square, mean, variance, kurtosis, crest factor, peak to peak, auto correlation and cross correlation) related to the monitored variables (e.g., temperature, electrical potential, corrosion current, mechanical stress and solution concentration) used to measure dissipative processes and consequent entropy value, detection and isolation of anomaly states by fault diagnosis approaches. The fault diagnosis approaches can include artificial neural network [107, 108, 83], wavelet theory [109, 110], relevance vector machine [111], support vector machine [112] order tracking method [113] and instantaneous power spectrum statistical analysis [114]. The third step includes the use of prognostic techniques (e.g., artificial neural network [82], fuzzy logic [115], wavelet theory [107], relevance vector machine [111], Bayesian methods (e.g., Kalman filter and particle filter [85, 86]), regression [116], demodulation [117], time series analysis [118] and fusion prognostics techniques [119]) for entropy-based damage model parameters estimation and prediction purposes.

The fourth and final step is RUL prediction. As discussed earlier endurance threshold determination is critical in the performance of RUL prediction [120, 88]. The entropy-based PHM framework suggested in this study handles the uncertainties related to endurance threshold by taking the advantage of entropy characteristics (e.g., providing the better estimate of degradation evolution, and being independent of the failure path as a thermodynamic state function).

5. Chapter 5: Entropic-Based Damage in Corrosion-Fatigue

Corrosion-fatigue is a coupled failure mechanism where two relatively independent degradation processes of corrosion and fatigue synergistically interact and accelerate the rate of damage, faster than otherwise realized by the sum of the two failure mechanisms. This chapter develops a thermodynamics model of the corrosion-fatigue failure mechanism, which will be used in the subsequent experimental observations as an example of a complex interactive failure mechanism. Accordingly, the main dissipative processes in the corrosion-fatigue failure mechanism are introduced and used to derive the total entropy generation function.

5.1 Main Dissipative Processes in Corrosion-fatigue

Figure 5.1 shows the setup for an experimental process that involves an aluminum specimen subjected to the corrosion-fatigue degradation mechanism. The specimen is electrochemically monitored. The corrosion process occurs at the surface of the specimen under a cyclic load with the following oxidation and reduction reactions for a metallic electrode, M:

$$M \leftrightarrow M^{z_M^+} + z_M e^- \tag{17}$$

$$O + z_O e^- \leftrightarrow R \tag{18}$$

where O is a certain oxidant in solution, which results in the formation of reduction product R.

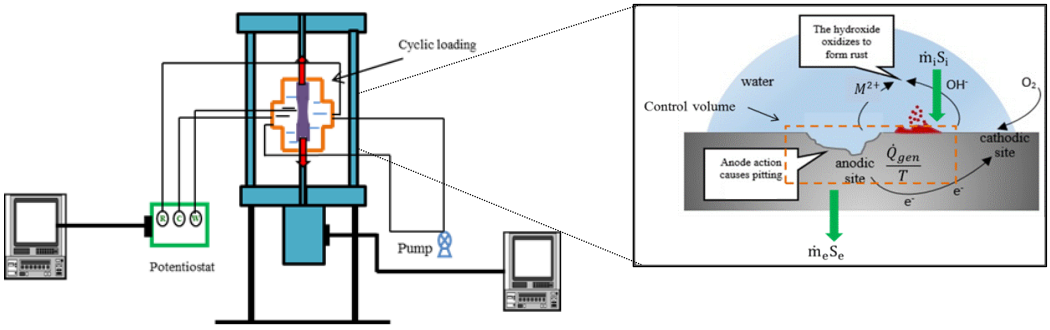

Figure 5.1. Entropy flow in the control volume under corrosion fatigue

Assuming a specific control volume, the main dissipative processes during the corrosion-fatigue failure mechanism include electrochemical losses induced by electronic current leakage (e.g. activation and Ohmic over-potentials); chemical reaction losses; mechanical losses; heat losses; and diffusion losses. According to Naderi et al. [59] and Ontiveros [52] the entropy generation due to heat conduction inside the solid is negligible in high-cycle fatigue. Assuming the corrosion fatigue in high-cycle regime and an adiabatic condition, the contribution of the corrosion activation over-potential, σ_{act}, corrosion reaction chemical potential, $\frac{1}{T}\Sigma_{j=1}^{r}\nu_j A_j$, diffusion over-potential, σ_{conc}, Ohmic losses, σ_{Ω} and mechanical losses, σ_M, on the rate of entropy generation for a control volume, can be determined by:

$$\sigma = \sigma_{act} + \frac{1}{T}\Sigma_{j=1}^{r}\nu_j\, A_j + \sigma_{conc} + \sigma_{\Omega} + \sigma_M \tag{19}$$

where the contribution of each term is explained in the following.

5.2 Activation Over-potential

Activation over-potential is the additional electric potential necessary to overcome the energy barrier in order for the electrode reaction to proceed at a desired rate. For example, when a cathodic over-potential, E, is applied to the electrode, the oxidation cathodic reaction rate is reduced and the oxidation anodic rate increases. This is accomplished by decreasing the activation energy for the cathodic reaction by an amount, $E_{M_{act,c}} = \alpha_M z_M F(E - E_{corr})$, and increasing that for anodic reaction by an amount, $E_{M_{act,a}} = (1 - \alpha_M) z_M F(E - E_{corr})$, where E_{corr} is the Open-Circuit Potential (OCP), and α_M is the charge-transport coefficient for oxidation reaction. Considering the irreversible fluxes of the anodic and cathodic half reactions of process 18, the contribution of the corrosion activation over-potential to the entropy generation for a control volume, V, can be expressed as:

$$\sigma_{act} = \frac{1}{T}\left(\boldsymbol{J}_{M,a} z_M F E_{M_{act,a}} + \boldsymbol{J}_{M,c} z_M F E_{M_{act,c}} + \boldsymbol{J}_{O,a} z_O F E_{O_{act,a}} + \boldsymbol{J}_{O,c} z_O F E_{O_{act,c}}\right) \quad (20)$$

where $\boldsymbol{J}_{M,a}$ and $\boldsymbol{J}_{M,c}$ are the irreversible anodic and cathodic activation currents for oxidation reaction, respectively, and $\boldsymbol{J}_{O,a}$ and $\boldsymbol{J}_{O,c}$ are the anodic and cathodic activation currents for reduction reaction, respectively. In the case of corrosion-fatigue, both anodic and cathodic polarization can influence the degradation mechanism, with different behaviors observed during crack initiation compared to crack growth, and for steels compared to either aluminum or titanium alloys [121]. For example, Duquette et

al. [26] reported that the fatigue lives of smooth specimens of Al-7075 and Al-Mg-Li in NaCl solution were reasonably low at both anodic and cathodic polarization. However, corrosion-fatigue of polished specimens of 1020 and 4140 steels exposed to NaCl during high-frequency rotating bending occurred only when a critical anodic current was surpassed [121].

5.3 Ohmic Over-potential

The current that passes between the working electrode and auxiliary electrode creates a potential gradient in the electrolyte. This effect is called Ohmic over-potential and is more pronounced at high current densities or in electrolyte solutions of low conductivity. To minimize the effect of Ohmic over-potential, the accepted method is placement of the Luggin capillary close to the working electrode.

5.4 Diffusion Losses

Concentration over-potential caused by the failure of the surrounding material to preserve the initial concentration of the bulk solution as a reactant is consumed at the electrode. Concentration over-potential for anodic oxidation during corrosion can usually be ignored because of the presence of an unlimited supply of metal atoms at the interface [29]. This loss process occurs over the entire range of current density but is predominant at high cathodic reactions, leading to depletion of the dissolved species

in the adjacent solution [122]. The contribution of the concentration over-potentials for cathode reaction, using a simplified approach based on Fick's law, can be obtained as:

$$\sigma_{conc} = \frac{1}{T}\left(\boldsymbol{J}_{M,c}E_{M_{conc,c}} + \boldsymbol{J}_{O,c}E_{O_{conc,c}}\right) \tag{21}$$

where $E_{M_{conc,c}}$ and $E_{O_{conc,c}}$ are cathodic oxidation and reduction diffusion over-potentials, respectively.

5.5 Mechanical Losses

The mechanical dissipative losses, σ_M, constitute plastic, $\dot{\boldsymbol{\epsilon}}_{\boldsymbol{p}}:\boldsymbol{\tau}$, and elastic energy losses. Plastic losses are explicitly associated with the total generated entropy as shown in Equation 10. When the material is under cyclic loading in the elastic region, consistent with the continuum mechanic rules, it does not experience any permanent deformation, and the stress-strain diagram goes back to the origin [41]. In other words, fatigue would not be possible under the elastic regime, which would violate the second law of thermodynamics. Inspection of the material at the atomic scale, however, shows that atoms do not necessarily return to their initial lattice site but to a lower energy level [123], which leads to the formation of nano-scale voids and stress concentration locations. As a result, these voids grow and coalesce to form micro cracks in the material. For the case of high cycle fatigue under elastic deformation, Ontiverous [52] and Temfack and Basaran [41] introduce irreversible entropy generation due to elastic work. Due to the mechanical nature of the fracture and crack propagation, we

categorize losses due to these degradation processes as resulting from mechanical losses.

Interactions between dislocations and the environment at the crack initiation points are commonly suggested as a source of degradation in corrosion-fatigue [121]. The hydrogen embrittlement hypothesis is supported by extensive but incidental evidence as an important mechanism for corrosion-fatigue crack propagation, and the hydrogen embrittlement hypothesis is the most readily acknowledged degradation mechanism for high-strength alloys in strong hydrogen-producing environments [124, 125, 126]. Hydrogen embrittlement results from the diffusion of hydrogen atoms (a byproduct of the corrosion process) into the lattice space of metals and alloys, which can weaken atomic bonds, causing de-cohesion of lattice bonds and enhancing localized plasticity through crack tip dissolution. Hydrogen-enhanced corrosion-fatigue cracking is either inter-granular or trans-granular, with the latter involving a dislocation of the substructure [121].

A thermodynamic model for hydrogen-enhanced anodic dissolution was first suggested by Qiao et al. [74]. Near-neutral stress corrosion cracking analysis in some studies [73, 127] has suggested the acceleration of anodic current due to hydrogen-facilitated free energy increments and strong synergistic interactions between the dissolved hydrogen and the local stress field around the crack tip. However, such a strong change in the free energy and synergistic effect is not supported by the experimental results found by other studies [128, 129, 130].

Another important mechanism for initiating cracks is when passive films are not capable of extensive plastic deformation relative to the underlying metal, which can cause corrosion-fatigue damage through one or more processes, including a reduction of near-surface plasticity, leading to reduced or enhanced corrosion-fatigue (depending on the cracking mechanism), localization of near-surface dislocation structure and voids, and film-induced cleavage [131, 132, 121]. These phenomena—along with others such as micro crack propagation [133, 134, 135], surface energy change [136], crack closure [137, 138], microstructure [139], crack size [140], and configuration of micro cracks and cavities—represent internal corrosion-fatigue processes requiring an advanced means of measurement by direct observation, and do not appear explicitly either in the law of conservation of energy or the second law of thermodynamics. The internal variables theory [45], an alternative approach to non-equilibrium thermodynamics, enables us to supplement local equilibrium variables (e.g. volume and deformation) with the corresponding scalar or tonsorial variables which represent these internal phenomena. It is beyond the scope of this study to analyze these phenomena by implementing internal variables, but benefitting from the entropy characteristic (i.e. being as a measure of uncertainty), their subsequent effects are considered in the stress-strain and corrosion potential-electrical charge hysteresis energy loops described in the next section.

5.6 Total Entropy Generation during Corrosion-fatigue

Using Equation 19, the contribution of the above factors to the entropy generated in a control volume can be expressed as:

$$\sigma = \frac{1}{T}\left(\boldsymbol{J}_{M,a}\alpha_M\tilde{A}_M + \boldsymbol{J}_{M,c}(1-\alpha_M)\tilde{A}_M + \boldsymbol{J}_{O,a}\alpha_O\tilde{A}_O + \boldsymbol{J}_{O,c}(1-\alpha_O)\tilde{A}_O\right) + \frac{1}{T}\left(\boldsymbol{J}_{M,c}E_{M_{conc,c}} + \boldsymbol{J}_{O,c}E_{O_{conc,c}}\right) + \sigma_\Omega + \frac{\dot{\boldsymbol{\epsilon}}_{\boldsymbol{p}}:\boldsymbol{\tau}}{T} + \frac{\sigma_{M_e}}{T} \quad (22)$$

where $\tilde{A} = \Sigma_i \nu_i \tilde{\mu}_i$ is electrochemical affinity induced by electrochemical potential $\tilde{\mu}_i = \mu_i + z_i F(E - E_{corr})$, and σ_{M_e} is the dissipative part of the energy resulting from elastic deformation of material.

6. Chapter 6: Experimental Approach and Results

To understand the underlying dissipative processes in a corrosion-fatigue failure mechanism, and to measure the resulting entropic damage, a number of corrosion-fatigue tests are designed and performed in the Probabilistic Physics of Failure and Fracture (P^2F^2) Laboratory of the Center for Risk and Reliability at the University of Maryland. This chapter describes the specimen design, the alloy and the experimental set up, and the procedures used to simulate a corrosion-fatigue failure mechanism. In a corrosion-fatigue mechanism, not only does the stress cause the flow of dislocation, but the anodic current present at the electrode surface can also increase the mobility of dislocation and reduce the resistance against plastic deformation [27]. This *cross coupling effect,* or synergistic effect, which is known as mechano-chemical effect, is supported by the experimental results presented in this chapter.

6.1 Specimen Design and Material

Corrosion damage is often formed on structural components exposed to fatigue loading. Maritime aircraft along with other types of naval vessels and structures subjected to sea water are susceptible to corrosion damage. The main structural alloy which constitutes the primary parts of airframes in service is 7075-T6xx, selected for its high strength properties. Hence, this study desires to investigate the effect of the corrosion-fatigue damage on this alloy from thermodynamic perspective.

The “as received” chemical composition of the cold-rolled alloy aluminum 7075-T651 being investigated is shown in Table 6.1. The specimen was designed using finite element analysis to ensure that failure occurred in the middle section with the width of 2 mm. The structural mechanics module of COMSOL software was used to perform a finite element analysis in which the specimen was analyzed under static tension load. In this simulation, the linear elastic model was used to describe the material. Figure 6.1 shows the 3D and 2D geometry of specimen.

Table 6.1. As received Al 7075-T651 composition

Composition	**Si**	**Fe**	**Cu**	**Mn**	**Cr**	**Ni**	**Zn**	**Ti**	**Mg**
% by weight	0.049	0.18	1.53	0.012	0.18	0.018	5.73	0.028	2.46

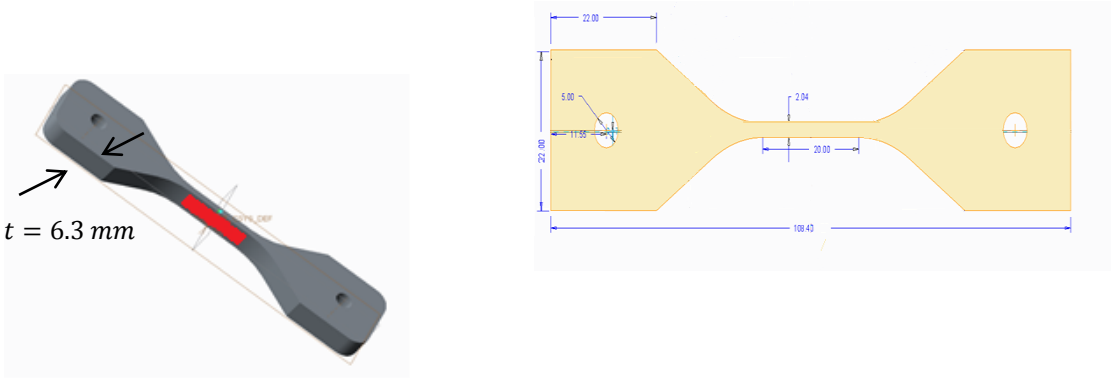

Figure 6.1. Specimen geometry (sizes are in mm)

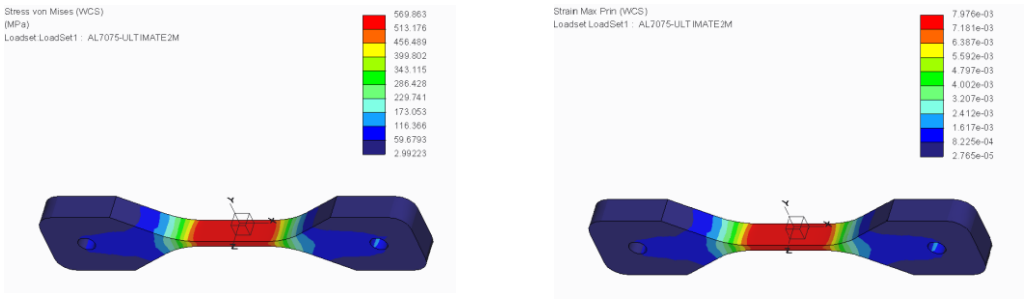

Figure 6.2. Specimen Finite element analysis

The Von Misses stress and strain distribution of the Al 7075-T651 specimen that underwent axial tensile loading with the maximum stress values in the center of the specimen are shown in Figure 6.2.

6.2 Experimental procedure

Fatigue tests were carried out in a corrosive 3.5% wt. NaCl aqueous solution, acidified with a 1 molar solution of HCl, with a pH of 3, under axial loading and load controlled under free corrosion potential. This concentration was selected to simulate the salinity of sea water, and the pH was selected based on electrochemical principles which indicate that aluminum is susceptible to corrosion at these conditions. The red area in Figure 6.1 shows the corrosion area. Before testing, the specimens were ground with SiC abrasive papers of grits up to #1200, then successively cleaned and rinsed with de-ionized water and acetone. The schematic of the experimental setup is shown in Figure 6.3a. The Instron software recorded mechanical stress and strain values. A digital image correlation technique [141] was also employed to validate Instron outputs. An

electrochemical corrosion cell, made from plexi-glass, was designed and built to be compatible with the whole gauge section of the specimen as shown in Figure 6.3b. The whole gauge section (the area of interest) of the specimen was electrochemically monitored using a Gamry potentiostat device with an Ag/AgCl electrode as the reference electrode (RE) maintained at a constant distance (2 mm) from the specimen, a platinum counter electrode (CE) and the specimen as the working electrode (WE). All the tests were conducted after the WE, immersed in the solution, reached the equilibrium OCP. The flow rate was approximately considered as zero.

Tests were carried out at the maximum cyclic stress, P, levels of 87%, 80%, 70%, 63%, 57%, 51% and 41% of the corroded specimen yield stress, stress ratio of 0.01, and loading frequency of 0.04 Hz. The waveform was sinusoidal. The stop criterion was the failure of specimens.

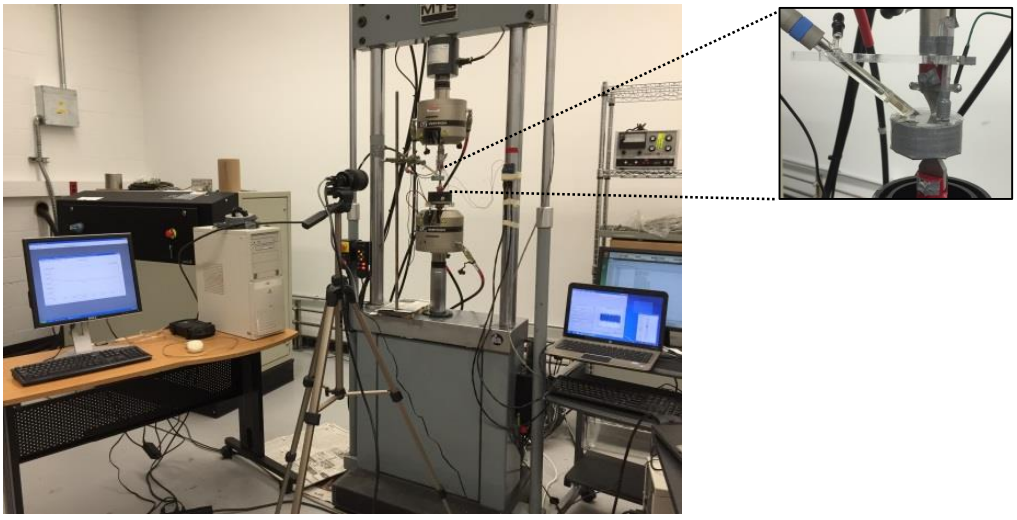

(a) (b)

Figure 6.3. Experimental setup

6.3 Tensile Mechanical Properties of Specimens in Corrosive Environment

Before the principle corrosion-fatigue tests were conducted, a tensile mechanical test was performed to obtain the mechanical and electrochemical properties of the specimen immersed in corrosive environment. Figure 6.4 shows the decrease of elongation to fracture of a specimen tested in the NaCl 3.5%wt. solution versus air. Alexopoulos et al. [142] show the same property for a tensile test of Aluminum 2024 in a corrosive environment. The yield and ultimate strength of the corroded specimen decreased by 20% when the tensile strength of the specimen was tested in air.

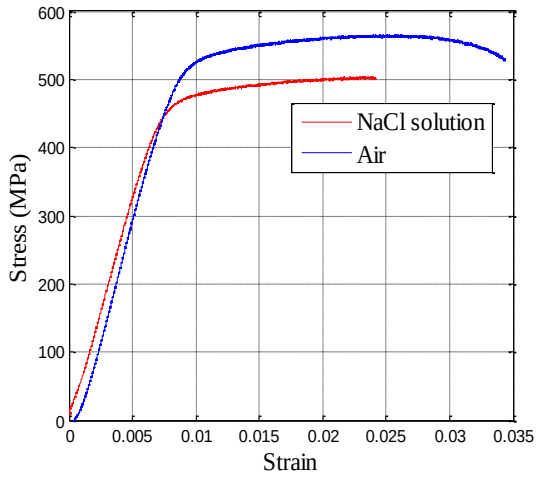

Figure 6.4. Tensile stress-strain curves for aluminum alloy 7075-T651 in air and NaCl 3.5% wt.

6.4 Experimental Observation of Synergistic Mechano-chemical Effect

The corrosion-fatigue tests were conducted while measuring the OCP variations during load-unload versus the unstrained RE. Figure 6.5 shows a dependence of OCP of a specimen under cyclic load as a result of mechano-chemical effect. According to the mechano-chemical effect, we can expect to observe an enhanced anodic dissolution flux induced by dynamic surface deformation. Meanwhile, the anodic current at the electrode surface can decrease near-surface work hardening and increase the mobility of dislocation, ultimately stimulating fatigue damage [29, 121, 30]. Gutman [29] and Sahal et al. [66] suggested that the local value of the chemical potential in the liquid-solid system is defined only by the absolute value of the hydrostatic part of the stress tensor, τ_m, and is independent of the deviatory part of the stress. Using the solid incompressibility hypothesis [29], the potential difference caused by stress is given by:

$$\Delta\phi = \frac{V_m \tau_m}{z_M F} \tag{23}$$

where V_m is the molar volume. It should be noted that the increase of the free energy due to the field stress only influences the potential of the ions in the metal, and not the potential of the metal ions in the electrolyte. If the Ohmic and concentration over-potentials are considered negligible, the dissolution current density can be expressed as [29]:

$$i = J_M^0 exp(\frac{V_m \tau_m}{RT}) exp\left(\frac{\alpha_M \tilde{A}_M}{RT}\right) - J_M^0 exp(\frac{(1-\alpha_M)\tilde{A}_M}{RT}) \quad (24)$$

where $exp(\frac{V_m \tau_m}{RT})$ expresses the effect of stress. In this study, the value of $\Delta\phi$ is obtained in a useful range, in accordance with the experimental results. For example, in Figure 6.5, where the maximum cyclic stress, $P = 330MPa$, is applied, the potential difference, $\Delta\phi = 0.002$v, is in good agreement with the value of $\Delta\phi$ obtained from Equation 23, where molar volume, V_m = 10 cm^3/mol, the hydrostatic part of the stress tensor, $\tau_m = \frac{1}{3}P$ [29] and $z = 3$ were considered for the anodic dissolution of the aluminum matrix [122, 143], which is believed to dissolve when it is immersed in 3.5% wt. NaCl solution. In order to understand the corrosion characteristics of Al7075, the constituent particles and corrosion morphology of Al 7075 are discussed in the next sections.

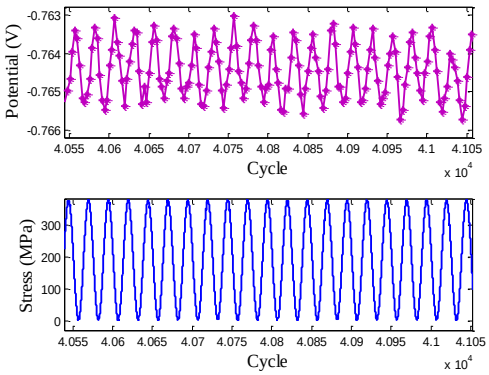

Figure 6.5. Open circuit potential variation during cyclic load application

6.5 Al 7075 Constituent Particles

In Al 7075, three types of constituent particles are present. The first type is Fe-containing constituent particles that have irregular shapes and sizes ranging from a few μm to 30 μm. Because these particles have a higher electrochemical potential than the surrounding Aluminum matrix and will act as cathodes in the presence of salt water, they are referred to as C-type particles. About 80% of the constituent particles seen in Al 7075 were C-type particles.

The second type of constituent particle in Al 7075 is Cu/Mg-containing particles as Al_2CuMg. Many of the Cu/Mg-containing constituent particles are spherical with a size ranging from a few μm to < 10 μm. Because these particles have a more negative corrosion potential than the Aluminum matrix and are referred to as A-type particles.

A few silicon-containing particles are in Al 7075. Their numbers are less than those of the other two types of particles, and they are electrochemically "neutral" relative to the Aluminum matrix, thus, do not appear to play a significant role in the pitting process [144, 145].

6.6 The Corrosion Attack Morphology of Al 7075

It has been shown that for Al 7075 in NaCl 3.5%wt. there is no appreciable attack on the matrix that surrounds C type particles [144]. However, at the A type particle sites, evident attack was observed [144]. It is believed that because of the more negative corrosion potential of these particles relative to the matrix they begin to dissolve when

they are immersed in 3.5% wt. NaCl solution. However, due to the selective dissolution of Mg in Al_2CuMg particles the remaining particles may become Cu-rich and cathodic relative to the matrix. Similar to what observed in the pitting corrosion of Al2024 [144]. In these cases, the surrounding matrix will be under corrosion pitting attack [145, 144]. The corrosion pit formation is related to the local breakdown of oxide layer. It has been shown that, pitting occurs at three steps, namely, adsorption of chloride ions on the anodic film, penetration of the aggressive anions into the anodic layer and initiation of corrosion process after electrolyte penetration. Comprehensive reactions during pitting corrosion of Aluminum in NaCl solution have been investigated by Gustavo et al. and Nguyen et al. [146, 147]. Basically, chloride ions are absorbed on the oxide film followed by the local break down of the film at weak points.

6.6.1 Anodic reactions

Initiated pits propagate through the dissolution of the Al ions as

$$Al = Al^{3+} + 3e^{-} \quad (25)$$

The dissolution of Aluminum by formation of Al^{3+} ions at the bottom of pit induces an electrical field that causes the adsorption of Cl^{-} species at the pit's bottom and forms a solid salt in pits to neutralize the solution and form Aluminum chlorides which followed by the dissolution of the adsorbed complex [143].

$$Al + Cl^- \rightarrow AlCl^- \quad (26)$$

$$AlCl^- \rightarrow Al^{3+} + Cl^- + 3e^- \quad (27)$$

Without any inhibitive species, water molecules promote the formation of an oxide layer, which is responsible for the re-passivation of an active pit.

$$2Al + 3H_2O \rightarrow Al_2O_3 + 6H^+ + 6e^- \quad (28)$$

Thus, in the pit there is a high concentration of hydrogen ions which causes an acidic environment within a pit and is mainly contributed to the dissolution of the oxide film as:

$$Al_2O_3 + 6H^+ \rightarrow 2Al^{3+} + 3H_2O \quad (29)$$

6.6.2 Cathodic reaction

The cathodic reaction can be considered as a four-electron O_2 reduction [143].

$$O_2 + 2H_2O + 4e^- \rightarrow 4OH^- \quad (30)$$

The above anodic and cathodic reactions are useful for simulation purposes which is not the focus of this research.

7. Chapter 7: Application and Demonstration of the Proposed Entropic-Damage Theory to Corrosion-Fatigue

7.1 Quantification of Entropy Generation in Corrosion-Fatigue

In this study, the corrosion-fatigue entropy generation was quantified based on the following assumptions: (1) the corrosion process occurs close to the equilibrium state (i.e., OCP), and the classical theory of irreversible processes does not cope with situations far from equilibrium; (2) entropy flow due to heat exchange is negligible in accordance with Naderi et al. [59] and Ontiveros [52], whose results showed insignificant entropy generation due to heat conduction inside the solid under high-cycle fatigue. Although the high-cycle fatigue does not result in significant heat conduction, low-cycle fatigue can experience noticeable thermal heat generation and conduction [148]; (3) diffusion losses are eliminated since the solution species are assumed to be well mixed; (4) the corrosion of the Al samples are considered as potential controled (5) the effects of diffusivity and concentration of hydrogen at the crack surface are excluded from entropy calculation because, for aluminum alloys under cyclic loading in the sodium chloride solution, Mason [8] indicates that above a critical frequency of load cycling (of 0.001 Hz), shorter cycle periods provide less time for diffusion and accumulation of hydrogen; (6) the Ohmic over-potential can be ignored, as its effect was minimized by placement of the Luggin capillary close to the working electrode; and (7) the corresponding current to OCP records can be obtained based on the fit of the sum of two exponential functions to the part of the polarization

curve where OCPs vary (i.e., around the second breakdown potential) in the corrosion-fatigue experiments (refer to Figure 7.1a and Figure7.1b). In order to explore the effect of corrosion time and cyclic loading on the polarization behavior, a potentiodynamic scan was performed at different loads and immersion time periods, as represented Figure 7.1a and Figure 7.1c. Since the results show no particular patterns in the variation of polarization curves with alteration of load conditions and immersion times, the mean of the polarization curves with a greater range of uncertainty (Figure 7.1a) was used for corrosion current evaluation.

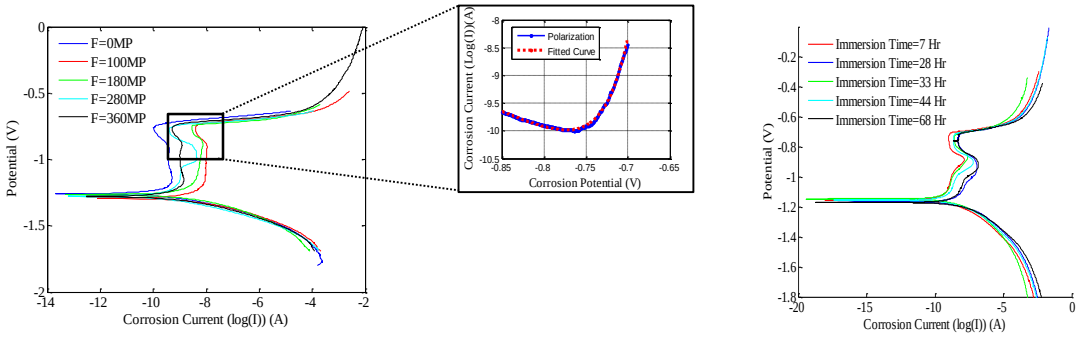

(a) (b) (c)

Figure 7.1. (a) Polarization curves at different stress levels (b) the corrosion current as a function of potential was obtained by fitting the sum of two exponential functions to the interval of potential values corresponding to OCP variations during corrosion-fatigue tests (c) polarization curves after different immersion time periods.

The above assumptions allow us to eliminate the effect of heat conduction, diffusion, hydrogen embrittlement, and Ohmic over-potential due to their insignificant contributions to entropy generation. The amount of entropy generated in each cycle of the corrosion-fatigue experiment is then obtained in terms of the area of the hysteresis energy loops resulting from mechanical stress-strain [56] and the energy resulting from variation of corrosion potential-current in each cycle of loading and unloading. Results are shown in Figure 7.2.

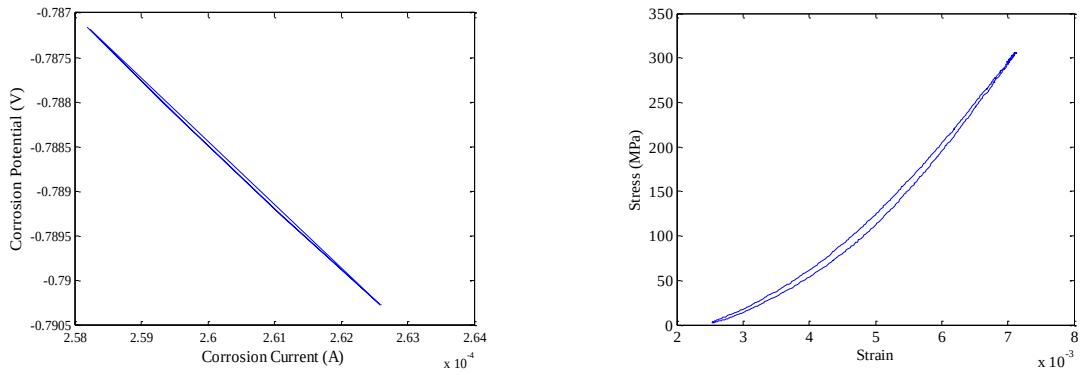

Figure 7.2. Corrosion potential-current and stress-strain hysteresis energy loops

Table 7.1 contains the conditions and results for the corrosion-fatigue experiments, including the stress magnitudes, the loading ratio, the frequency, entropy to failure values for corrosion and fatigue and the cycles to failure. In order to take into account the effect of variabilities and uncertainties, each test condition was applies to a group of at least four specimens. Additionally, two sets of tests were performed at the maximum cyclic stress chosen as 51% and 41% of the corroded specimen yield stress.

These supplementary tests were conducted to support the results of the tests with higher magnitude of stress.

Table 7.1. Corrosion-fatigue experiments results (the specimens marked with stars are used as training samples for RUL predictions)

Sample Number	**Maximum Stress(Mpa)**	**Loading ratio**	**Frequency (Hz)**	**Corrosion Entropy Value (MJ/Km^3)**	**Fatigue Entropy Value (MJ/Km^3)**	**Cycle to Failure (Cycle)**
1*	405	0.01	0.04	0.08	0.77	4811
2*	405	0.01	0.04	0.10	0.83	6114
3	405	0.01	0.04	0.12	0.91	7203
4	405	0.01	0.04	0.12	1.04	7309
5	365	0.01	0.04	0.08	1.03	5036
6*	365	0.01	0.04	0.11	1.07	6808
7*	365	0.01	0.04	0.15	1.27	9208
8	365	0.01	0.04	0.12	1.06	7175
9*	365	0.01	0.04	0.11	0.73	6683
10	330	0.01	0.04	0.16	1.06	9769
11	330	0.01	0.04	0.17	0.96	10189
12*	330	0.01	0.04	0.18	0.97	10539
13*	330	0.01	0.04	0.21	1.06	12647
14	330	0.01	0.04	0.21	1.13	12175
15*	295	0.01	0.04	0.16	0.84	9390
16	295	0.01	0.04	0.13	0.79	7635
17*	295	0.01	0.04	0.21	1.13	12620
18	295	0.01	0.04	0.18	1.33	10539
19*	265	0.01	0.04	0.34	1.2	19822
20	265	0.01	0.04	0.19	0.71	11383
21*	265	0.01	0.04	0.24	0.85	13943
22	265	0.01	0.04	0.1	0.60	7839
23	215	0.01	0.04	0.45	1.26	20739
24	190	0.01	0.04	0.48	1.21	27609

Figure 7.3a presents the evolution trend of corrosion-fatigue volumetric entropy for different loading conditions. The results show that the cumulative entropy values at the fracture points remain between 0.7 $MJm^{-3}\,K^{-1}$ and 1.7 $MJm^{-3}\,K^{-1}$. Figure 7.3b presents

the box plot of the fracture entropies at each loading condition, revealing that the mean of the fracture entropy values remains roughly 1.15 $MJm^{-3}K^{-1}$ with standard deviation of 0.2. This value can be taken as a very rough value of entropic-endurance. It is very rough because it is related to an observed marker of damage, and in our theory we note that cumulative entropy and entropic-endurance describe damages both observable and non-observable. However, for demonstration purposes, this would be tolerated, and we note that it will be a source of additional uncertainty and discrepancy in the results.

The slim distribution of entropy to failure data points demonstrates the ability of entropy to treat the uncertainties associated with microstate variabilities. Furthermore, it reveals that entropy is independent of the loading conditions. The entropy distribution at the fracture points is an expression of variabilities and uncertainties in experimental measurement errors, the legitimacy of the assumptions considered in developing the entropy evaluation, weaknesses in the control of the variables during the experiment, and variations in operational and environmental conditions. One important source of uncertainty is the assumption that the evaluation of damage is quantified relative to a negligible initial damage.

Figure 7.4a presents the normalized corrosion entropy with respect to the normalized fatigue entropy, where normalized entropies were calculated by dividing the entropy resulting from corrosion and fatigue, respectively, to the total entropy gain at the final fracture for different loading conditions. The result, interestingly, suggests that the normalized corrosion entropies increase monotonically with decreases in load, compensating for the decreases in fatigue entropy. Figure 7.4b represents the average

of specimens' corrosion to fatigue (CF) ratios at fracture points for different loading conditions. Using a second order polynomial to fit to the data (with the coefficient of determination, R^2equal to 0.96) obtained from experimental observations; the ratio of CF for lower mechanical loads can be estimated through extrapolation. Although extrapolation is subject to uncertainty—as the graph shows the CF ratio of one at the load of around 30 MPa— the graph can be used to approximately predict CF ratios at lower mechanical loads.

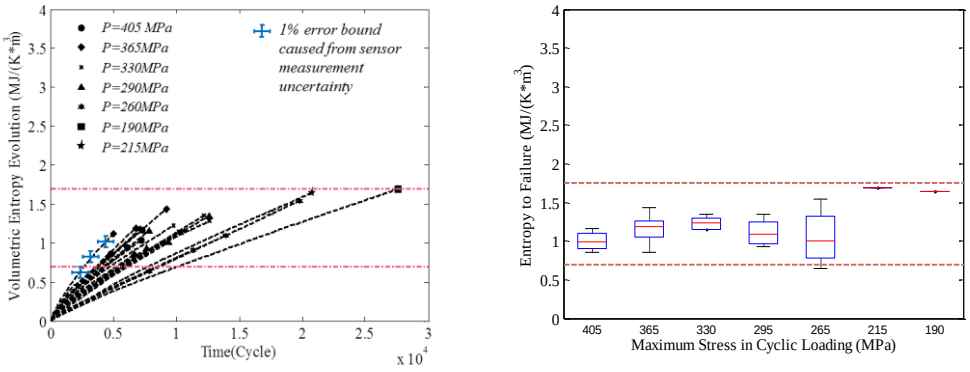

(a) (b)

Figure 7.3. (a) Cumulative entropy evolutions at different loading conditions, (b) Box plot of fracture entropies (entropy to failure) at each loading condition where boxes represent the interval of fracture entropy distributions, and mid lines reflect the mean of fracture entropies at each loading condition

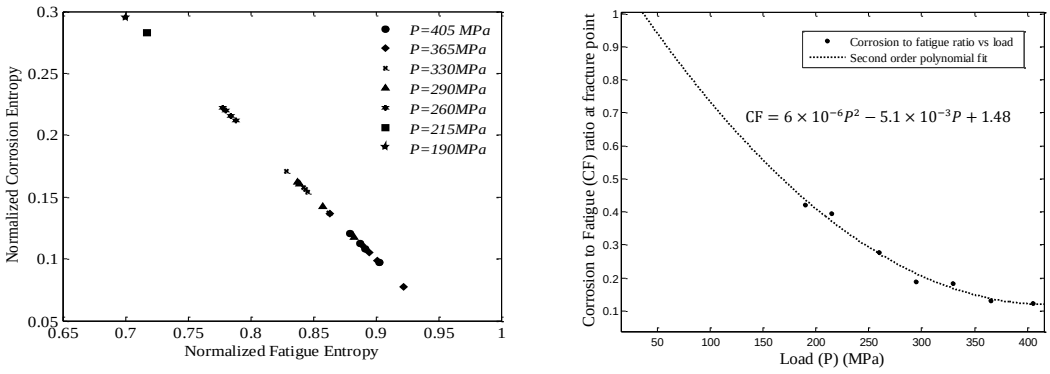

(a) (b)

Figure 7.4. (a) Normalized corrosion entropy versus normalized fatigue entropy, (b) Regression and extrapolation of the second order polynomial curve fitted to the experimental data

Using $\gamma_{d_E} = 1.15\ \mathrm{MJm^{-3}\ K^{-1}}$ as the mean of facture entropies for training samples described in the next section and $\gamma_{d_0} = 0$, the evolution trend of normalized cumulative volumetric entropy generation (i.e., the damage metric) for the Al specimens is shown in Figure 7.5.

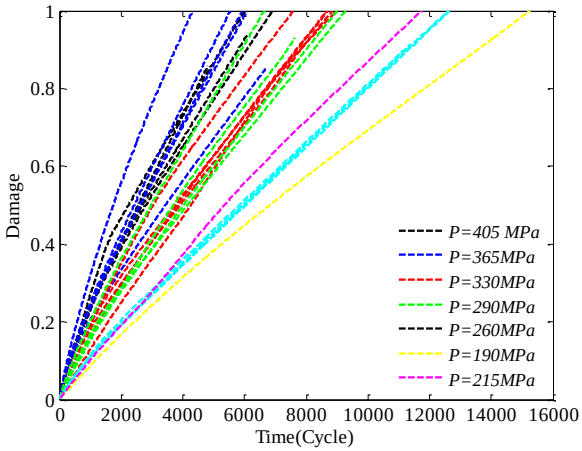

Figure 7.5. Damage evolution for Al samples undergoing the corrosion-fatigue degradation mechanism

7.2 Entropic Based Reliability Assessment within Corrosion-Fatigue

Using Equation 15 and the linear relationship between the cycle's evolution and cumulative entropies resulting from corrosion-fatigue experiments shown in Figure 7.5, the cycle to failure (CTF) PDF ($g(n)$) can be derived in terms of EDTF PDF ($f(D)$) as expressed in Equation 31. Note that in Equation 31, the number of cycle, n, represents "time".

$$g(n) = \gamma + \frac{\lambda}{\gamma n^2} f\left(\frac{\lambda}{\gamma n}\right) \tag{31}$$

where $\gamma = 1/t_c$ and $\lambda = D_f$ are the CTF distribution parameter. Herein, the assumption is that the point of "failure," which is an observed marker of damage, corresponds to the entropic-endurance level. Accordingly, the entropic-endurance level is selected as the mean of the total volumetric entropy generation at fracture points. This subjective choice is used for demonstration purposes only and would be the likely source of one of the main discrepancies between the actual EDTF PDF and derived EDTF PDF.

Figure 7.6 represents how the CTF PDF can be derived by applying Equation 31 to the EDTF PDF, depicted in Figure 7.6b. Thin distribution of EDTF in Figure 7.6b supports the entropy ability in handling the uncertainties to an appropriate extend. While the empirical distribution of EDTF would be adequate, one could also acquire known distribution models that fit well into the EDTF data. It reveals that the Weibull distribution fits reasonably well to the corrosion-fatigue EDTF data points obtained in these tests at the failure time, t_c, with a coefficient of determination, R^2, of 0.92. By substitution of Weibull distribution in Equation 31, the CTF PDF can be derived accordingly. To indicate the goodness of fit of Weibull distribution to the derived CTF PDF, the sum of square error between the derived PDF and the true CTF PDF (refer to Figure 7.6c) is calculated as of 0.0008. Furthermore, using the t distribution-test hypothesis to examine the null hypothesis that the two distributions (i.e., the true CTF PDF and derived CTF PDF) are from the same Weibull population with equal scale parameters at 5% significant level, results in the output of 0 and P-value equal to 0.9867, thus indicating that t distribution-test does not reject the null hypothesis. Based

on the derived CTF PDF the reliability of the specimens was estimated as 63%. In these calculations, t_c is selected as the mean of CTF (9493 cycle) data points.

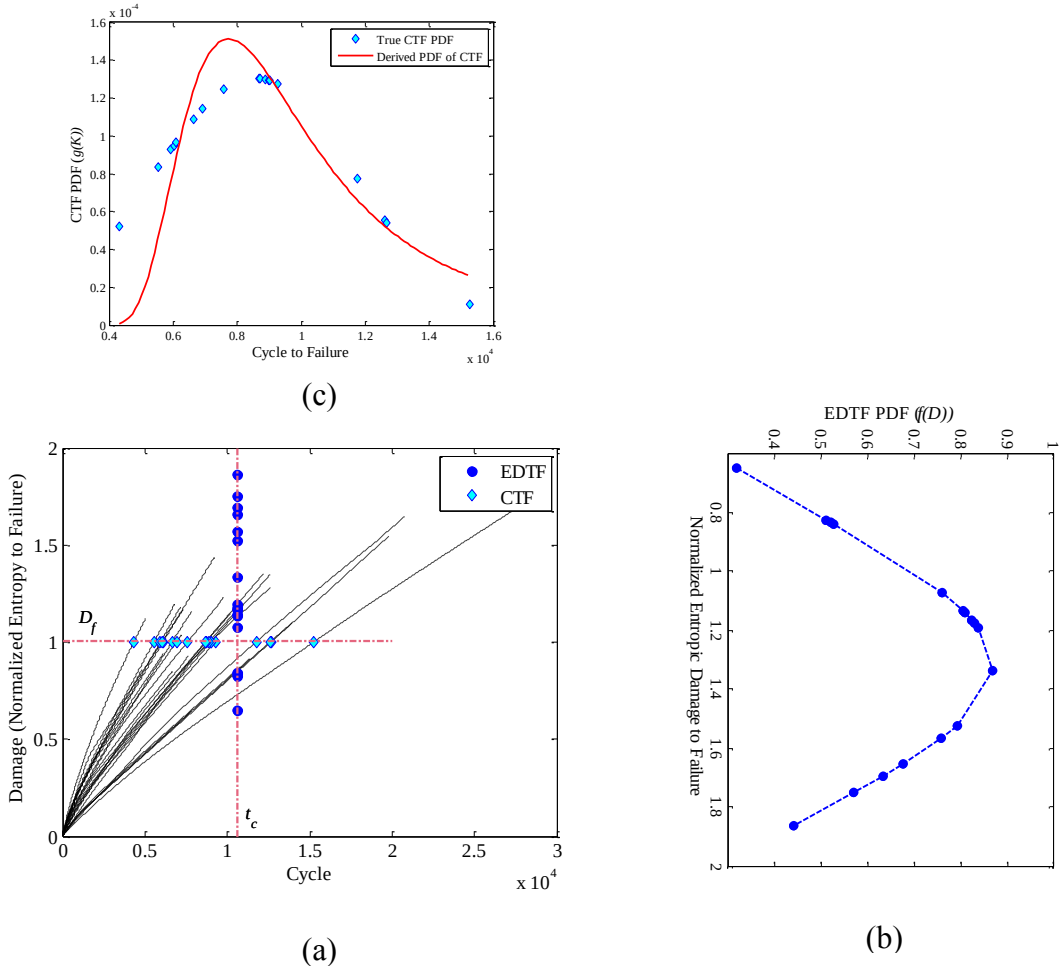

Figure 7.6. (a) Normalized entropy evolution of aluminum specimens; filled diamond and filled circles show the CTF and EDTF, respectively, (b) Weibull distribution function was fitted to the EDTF and (c) derived PDF of CTF based on EDTF PDF versus true CTF distribution

7.3 RUl Prediction by Entropic-Based PHM Framework

Figure 7.7 shows the implementation of the entropy-based PHM framework to the corrosion-fatigue degradation mechanism. The health assessment and RUL estimation of aluminum samples is demonstrated in two steps using two well-known methods in PHM. These steps are offline data analysis, including processing of training data such as extraction of features and classification of training data points to healthy and faulty labels, and online data analysis, including health assessment of test data points, estimation of online degradation model parameters and RUL prediction. The details of each phase are discussed below:

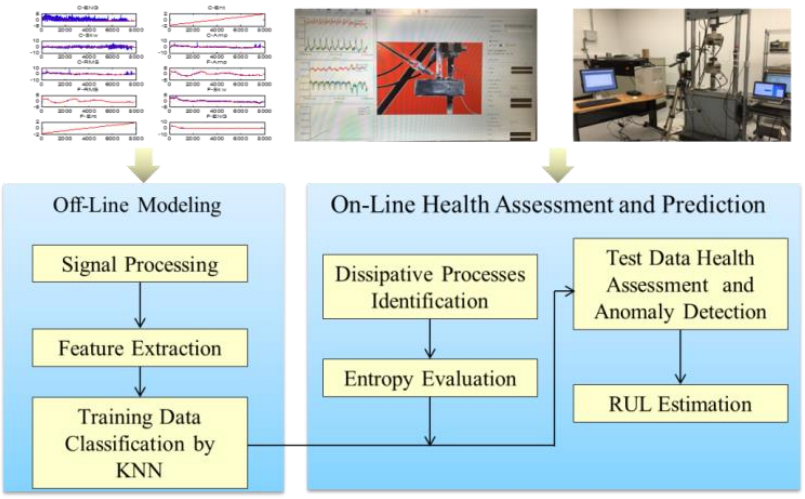

Figure 7.7. The application of the entropy-based PHM approach

7.3.1 Offline modeling

Assuming the corrosion and fatigue are the main dissipative processes, features of strain and corrosion potential variations (i.e. maximum amplitude, root mean square, and skewness) along with energy loop values resulting from stress-strain hysteresis and corrosion potential-electrical charge were processed for training samples. The training samples are marked with star superscript in Table 7.1. To evaluate the state of the components' health, the k-nearest-neighbor (kNN) [149] approach was employed. The kNN approach is a non-parametric classification method in which a new data point is classified based on its vicinity to the k neighboring data points of known classes. In this method, the Euclidean distance is calculated from a new data point to the centroid of the nearest neighbors from each class, and the new data is classified to the shortest centroid distance. The healthy and faulty classes were selected based on the portion of the specimen life. Data from the initial 10-30% and 70% lifetime defined the healthy and faulty class, respectively.

In kNN the selection of k is subject to the type of data. To obtain a proper value of k at which the classification output is stabilized, sensitivity analysis should be performed. In this study, the impact of the presence of noise in the classification was examined in altering the location of the nearest neighbors' centroid. In the sensitivity analysis, the change in the distance of a test point to the centroid of the nearest neighbors was calculated as the value of k was increased by one at each step, as shown in Figure 7.8. k was selected such that enough neighbors were selected to produce a stable neighbor's centroid.

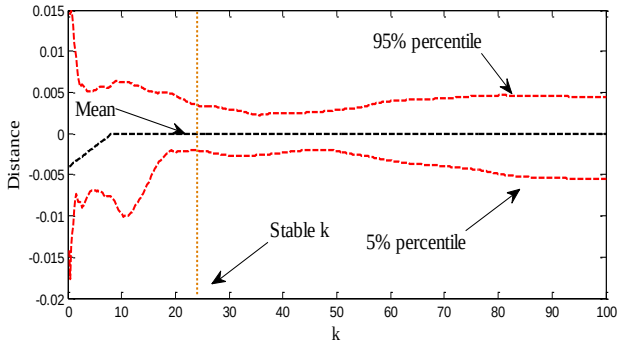

Figure 7.8. Selecting k based on sensitivity study for the training data

Fault level (FL) is determined by taking a moving average of the kNN binary output over time with a window of 100 data points. This enables the definition of anomaly detection threshold. An anomaly was acknowledged when the FL > 0.7. Based on the faulty portion of the lifetime, this threshold is defined as a minimum operating requirement level for an item (the item may still be operational, but not satisfactorily). The classification output plot is depicted for sample number 5 in Figure 7.9.

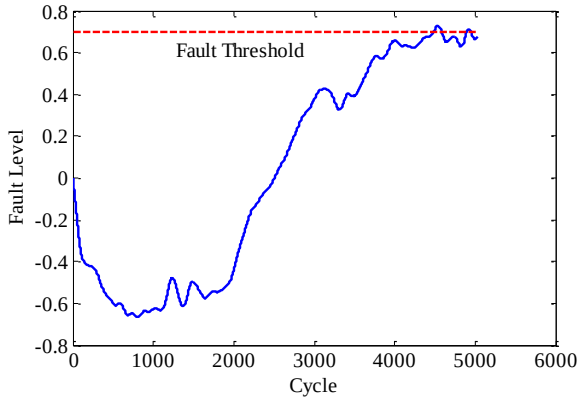

Figure 7.9. kNN classification output for sample number 5

7.3.2 Online modeling

By choosing the normalized volumetric entropy parameter as the index of damage to be monitored, the Bayesian updating method can be used to estimate the parameters of the degradation model and to predict age. The Bayesian updating approach provides a general, rigorous method for dynamic state estimation problems. The idea is to build a PDF of the system model states (i.e. the degradation model parameters in this study) based on all available information. Particle filter (PF) is a method for implementing a recursive Bayesian filter using Monte Carlo simulations. Herein, it approximates the damage evolution trends (depicted in Figure 7.5) parameters' PDF by a set of particles sampled from the normal PDF and a set of associated weights denoting probability masses [85].

As the particle filter requires models developed from known system behavior, the particles in the PF method are generated and recursively updated by system states evolution model shown in Equation 32, where the random walk model is considered for evolution of degradation trend parameters a_{0_n} and a_{1_n}, a measurement model depicted in Equation 33, and an *a priori* estimate of the system model states PDF.

$$a_{0_n} = a_{0_{n-1}} + \omega_{a_0}$$
$$a_{1_n} = a_{1_{n-1}} + \omega_{a_1} \quad (32)$$

$$D_n = a_{1_n} n + a_{0_n} + \theta \quad (33)$$

where $\boldsymbol{x}_n = [a_{0_n}, a_{1_n}]$ is the degradation trend parameter vector at cycle *n* while its elements are subject to normal distribution error, $\omega_{a_i} = Normal(0, \beta_{a_i}),\ i = 1, 2,$ with zero mean and standard deviation, β_{a_i}. D_n is the entropic damage measurement at cycle *n* which is subjected to a Gaussian noise, $\theta = Normal(0, \beta_D)$, and its progress model is obtained from the linear regression of damage trends depicted in Figure 3, with the average of coefficient of determination, R^2 equal to 0.98, estimated from the training samples' degradation evolution trends regression.

The goal of PF implementation is then to estimate the probability distribution of the degradation model parameters, a_{0_n} and a_{1_n}, given a series of entropic damage measurements, $D_n = [D_1, D_2, D_3, \dots, D_n]$. The particle filter is implemented by initiating the degradation model parameters by a set of particles, $\boldsymbol{x}_0^i$, where $i = 1, 2, \dots, N_s$.

Within the Bayesian framework, the posterior PDF of the system model states, $P_r(\boldsymbol{x}_{0:n}|D_{1:n})$, at cycle n can be approximated by:

$$P_r(\boldsymbol{x}_{0:n}|D_{1:n}) \approx \Sigma_{i=1}^{N_s} w_n^i \delta(\boldsymbol{x}_{0:n} - \boldsymbol{x}_{0:n}^i) \tag{34}$$

where $\delta(.)$ is the Dirac delta function, $\boldsymbol{x}_{0:n}$ and $D_{1:n}$ are the set of all states and damage measurements up to cycle n, and $\boldsymbol{x}_n^i,\ i = 1, \dots, N_s$, is a set of random samples drawn from $P_r(\boldsymbol{x}_{0:n}|D_{1:n})$ with associated weights $w_n^i, i = 0, \dots, N_s$, normalized such that $\sum_{i=1}^{N_s} w_n^i = 1$.

Sampling / importance resampling is a commonly used algorithm to attribute importance weight, w_n^i, to each particle, i, as:

$$w_n^i = \frac{P_r\left(D_{1:n}\middle|\boldsymbol{x}_n^i\right)P_r\left(\boldsymbol{x}_n^i\right)}{\pi\left(\boldsymbol{x}_n^i\middle|D_{1:n}\right)} \tag{35}$$

A recursive formulation in order to update the weights can be obtained as:

$$w_n^i = w_{n-1}^i \frac{P_r\left(D_n\middle|\boldsymbol{x}_n^i\right)P_r\left(\boldsymbol{x}_n^i\middle|\boldsymbol{x}_{n-1}^i\right)}{\pi\left(\boldsymbol{x}_n^i\middle|D_{1:n}\right)} \tag{36}$$

where the importance distribution $\pi\left(\boldsymbol{x}_n^i\middle|D_{1:n}\right)$ can be approximated by $P_r\left(\boldsymbol{x}_n^i\middle|\boldsymbol{x}_{n-1}^i\right)$, which is an arbitrarily chosen distribution [85].

7.3.3 RUL prediction

As discussed earlier, given a series of measured entropic damage values, D_n, the PF technique enables the estimation of the degradation model parameters (a_{0_n} and a_{1_n}), where in the updating process, N_s samples are used to approximate the posterior PDF of them. Each sample denotes a candidate for the system model state vector, $\boldsymbol{x}_n^i = [a_{0_n}, a_{1_n}]$, $i = 1, 2, \ldots, N_s$, so the prediction of damage, D, would have N_s possible

trajectories with the corresponding importance weight w_n^i. The l^{th} step ahead of the prediction of each trajectory at cycle n is calculated by:

$$D_{n+l}^i = {a_1}_n^i(n+l) + {a_0}_n^i \tag{37}$$

The estimated PDF of the damage prediction, $h(D)$, at l^{th}step ahead can be estimated by:

$$h(D) = P_r(D_{n+l}|D_{0:n}) \approx \sum_{i=1}^{N_s} w_n^i \delta(D_{n+l} - D_{n+l}^i) \tag{38}$$

where w_n^i kept constant with the corresponding values at the anomaly point. Defining a deterministic entropic endurance which corresponds to endurance threshold level as $D_f = 1$, the RUL probability estimation, R_n^i, of the i^{th} trajectory at cycle n can be obtained by solving the following equation as:

$$1 = {a_1}_n^i(n + R_n^i) + {a_0}_n^i \tag{39}$$

The PDF of the RULs at cycle n can be approximated by:

$$P_r(R_n|D_{0:n}) \approx \sum_{i=1}^{N_s} w_n^i \delta(R_n - R_n^i) \quad (40)$$

However, if the variability in the endurance threshold is considered with the PDF distribution $b(D_f)$, being independent from the deterioration distribution [150], the RUL cumulative density function at cycle n can be derived from Equation 41 which accounts for the knowledge of the deterioration state D_n at cycle n [150]:

$$RUL(n) = \int_{D_n}^{\infty} \frac{B(D) - B(D_n)}{1 - B(D_n)} h_{D-D_n}(D - D_n) dD \quad (41)$$

where B is the Cumulative Density Function (CDF) of the endurance thresholds (satisfying $B(0) = 0$), h_{D-D_n} is the probability of having at cycle n a deterioration increments $D - D_n$, and the term $\frac{B(D)-B(D_n)}{1-B(D_n)}$ is the left-truncated CDF of the endurance threshold providing the probability of having the endurance threshold between the current deterioration state (Anomaly point) and infinity.

7.3.4 Prognostics results

Using the kNN classification method, anomalies were identified when the test data FL crosses the anomaly detection threshold. Once the anomaly was detected, the PF algorithm was initiated to predict the RULs. The initial values of the degradation evolution trend parameters (a_{0_n} and a_{1_n}) were obtained from the least square

regression of degradation trend, using the healthy interval of the data for each test specimen. These parameters were updated by the PF algorithm in each cycle step. Figure 7.10a shows the prediction results for sample number 5. The left-truncated endurance threshold and the PDF of the predicted total life are shown in the red contour plot and blue line, respectively. Figure 7.10.b shows the distribution of the degradation trend at the anomaly criteria, resulting from the degradation model parameters uncertainties.

The same procedure was applied to the remaining specimens. The percentage of the mean of the predicted RULs and actual RULs, and the minimum and maximum absolute value of error between the predicted RULs at different endurance thresholds and actual RULs are shown in Table 2. The error interval falls in the range of 0.1% to 25.5%. This implies that using entropy as a measure of damage can handle the uncertainties related to the endurance threshold to a good extent. The performance of predictions, however, can be enhanced by reducing the uncertainties discussed earlier. Other studies such as [151, 88] suggest statistical solutions to manipulate the endurance threshold uncertainty in predicting the RUL, or using the opinion of experts with expertise within the relevant field to provide useful information about the threshold probability distribution. With the use of entropy as a damage index, however, this study tried to provide a practically scientific approach to control the endurance threshold uncertainty effects on RUL prediction.

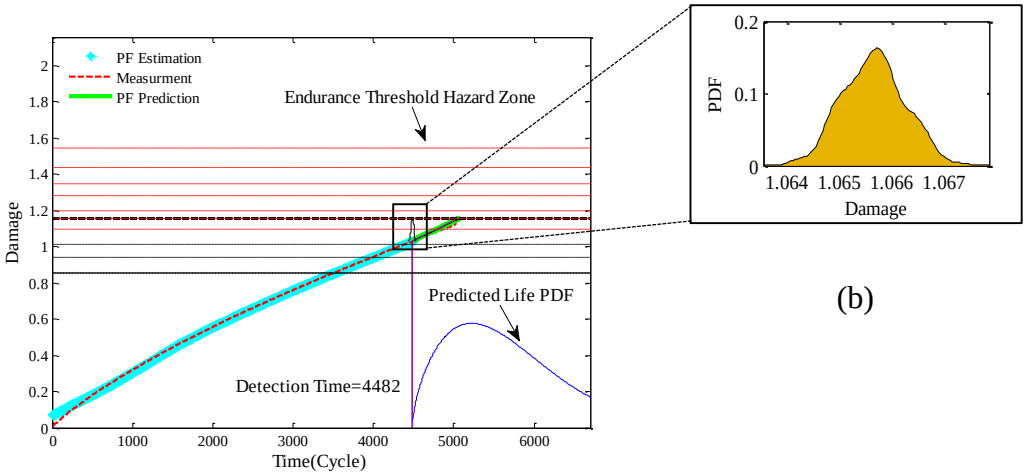

Figure 7.10. (a) RUL prediction for sample number 5, (b) distribution of degradation trend at the anomaly criteria

Table 7.2. RUL prediction results

Test sample number	Stress (MPa)	Actual RUL (% of life)	Mean of estimated RULs (% of life)	Error between actual RUL and mean of estimated RULs (% of life)	Minimum error between actual RUL and estimated RULs (% of life)	Maximum error between actual RUL and estimated RULs (% of life)
3	405	32.3	37.1	4.8	1.2	21.5
4	405	32.8	28.3	4.4	1.9	12.8
5	365	11.0	11.7	0.7	0.1	23.9
8	365	23.3	20.2	3.1	0.3	23.3
10	330	26.3	17.8	8.5	0.2	13.3
11	330	30.8	30.3	0.5	0.1	11.5
14	330	23.2	8.15	15.4	1.4	23.2
16	295	31.6	42.5	10.9	2.5	25.5
18	295	30.0	15.4	14.6	0.1	24.1
20	265	28.9	33.6	4.7	1.2	24.2
22	265	31.5	35.7	4.2	0.2	15.7

8. Chapter 8: Conclusions and Recommendations

8.1 Conclusions

This dissertation proposes a new entropic theory of damage that describes an index of damage on the basis of the generated entropy during any degradation process and describes and derives integrity and reliability expressions of critical components and structures within the irreversible thermodynamic framework. It suggests that the true damage in nearly all degradation processes is larger than the observed markers of damage, and if all degradation processes related to the failure mechanisms were known, the associated entropy generation from each mechanism would have been the true indicator for the total damage incurred, regardless of whether or not the damages were observable. Therefore, a unified "non-empirical" index of damage can be defined based on the entropy generation concept, which is capable of capturing the effects of multiple competing and interacting failure mechanisms, and can provide a consistent definition at a long stretch of scaling from micropscopic to macroscopic scales. The ability of entropy as a measure of uncertainty is described in terms of providing the best estimate of degradation accumulation and performance decline in the absence of any microstructural observation. Furthermore, it shows that entropy as a thermodynamic state function is independent of the failure path, and is capable of handling the uncertainties related to a metric defined as the entropic-endurance beyond which a failure will occur.

Using entropy as an index of damage, which relies on the most fundamental law of engineering and science (i.e., the second law of thermodynamics), proved useful to formally describe the reliability assessment of critical components and structures. It has been described that manufacturing imprecision, usage disparities, variabilities related to material properties, geometries or loading conditions and other events leading to damage impose uncertainties on the damage trends (i.e., normalized total entropy growth as the index), D, and resulting time to failure (TTF). This research provided a formalism to relate the entropy-based damage to the corresponding reliability models of life. Deriving the reliability function in terms of the entropic damage to failure probability distribution function, and knowing the contributions of different dissipative processes in form of entropy generation, can offer a foundation for other applications (e.g., prognosis and health management) in structural integrity assessment.

The application of the entropic-based damage is also demonstrated within the prognosis and health management framework to estimate remaining useful life prediction of critical components and structures within the irreversible thermodynamic framework. The suggested approach not only offers a science-based foundation for PHM methods, but also benefits from the superior advantages of the use of entropy as a damage index, in contrast with the common observable markers of degradation. In fact, the proposed entropic based PHM approach is preferred as it allows inclusion of all degradation mechanisms through quantification of entropy, based on failure mechanisms. With the use of entropy as "as measurement of uncertainty" for damage characterization, better estimates can be achieved with greater confidence. This entropic based approach

improves the performance of remaining useful life assessment by providing an almost constant entropic-endurance threshold. Furthermore, by decreasing the dimensionality of calculation better resource management can be optimized.

To evaluate the practicality of the approach for reliability analysis and integrity characterization, the entropic-based damage approach was implemented in corrosion-fatigue degradation mechanism, simulated in a laboratory environment. Using this theorem, which relates entropy generation to dissipative phenomena and under the assumptions mentioned earlier, the thermodynamic entropies generated in the corrosion-fatigue degradation mechanism of dog-bone samples exposed to simultaneous cyclic loading and corrosive environment was evaluated in terms of the associated dissipative processes. With the elimination of the effect of heat conduction, diffusion loses, hydrogen embrittlement dissipations and Ohmic over-potential due to their insignificant contributions to entropy generation, the main entropy contributions are assumed to be the result of corrosion and fatigue degradation processes. It has been shown that using the concept of entropy-based-damage can alleviate the conceptual challenges when dealing with different degradation mechanisms (i.e., corrosion and fatigue in corrosion-fatigue failure mechanism) with different observable markers, which allows us to provide a consistent definition of damage. For example, materials removal owing to corrosion may be viewed as a surface damage, while in fatigue the change of strain in material may be used as a volumetric damage. However, as far as both degradation processes occur in the same control volume, their entropy generation contributions can be added to indicate the entirety of the damage incurred.

The synergistic mechano-chemical effect arising from interaction of synergistic corrosion and fatigue processes was revealed within experimental records. The amount of chemical over-potential enhanced by cyclic stress was shown to be in good agreement with the value of chemical over-potential induces by mechanical load obtained in literature.

The experimental results showed that the cumulative entropy generations resulted in corrosion-fatigue tests at the time of failure, while scattered due material-to-material variability, remain approximately constant and are independent of the loading conditions. This result supports the proposed theory of entropic-damage being independent from failure path as a thermodynamic state function.

It was shown that the contribution from the cumulative corrosion entropy increased with the decrease of load (which corresponds to the decrease of fatigue entropy), but that the total cumulative entropy remained constant. Fitting a second order polynomial to the specimens' corrosion to fatigue ratios at fracture points for different loading conditions; it has been shown that the contribution of the corrosion and fatigue entropies for lower mechanical loads can be estimated through extrapolation. Using a linear relationship between cumulative corrosion-fatigue entropy and time evolution, the entropy-based damage reliability model was derived based on the relationship between the entropic damage to failure probability distribution function and cycle-to-failure probability distribution function. Using the t distribution-test hypothesis the dissertation confirmed the goodness of fit of derived cycle to failure probability distribution function.

An entropy-based prognostic and health management approach was also implemented for structures subject to the corrosion-fatigue degradation mechanism. The thermodynamic entropy generated in the corrosion-fatigue degradation mechanism was then used to predict the remaining useful life of AL 7075-T651 samples. The use of entropy for prediction purposes was shown to be effective in terms of capturing the amount of damage and expended life due to dissipative processes (i.e., corrosion and fatigue), and. The limited difference between actual remaining useful life and estimated ones reveals that using entropy as a measure of damage is effective in handling the uncertainties associated with the entropic-endurance.

Finally, it is worth to note that, this study is limited to some assumptions. Important ones are: elimination of some of dissipative processes with insignificant contributions to entropy generation in quantifying the entropy generated during corrosion-fatigue experiments; consideration of presence of no damage in samples at the beginning of the experiments; and limited control of laboratory environmental conditions due to the long period of experiments. These shortcomings can be addressed by means of high precision observation equipment and sensors, using the correlation between the rate of damage and damage at different stages of degradation for quantification of damage at time zero [152], and use of modern technologies and methods to control the laboratory environmental conditions for long lasting tests.

8.2 Recommendations for Future Work

The following areas are suggested for future research.

- Perform fatigue tests using a broader spectrum of stress amplitudes and loading ratios to improve the estimates and reduce uncertainties.
- Conduct spectrum loading to investigate the feasibility of applying an entropic-based damage approach to more complex and realistic degradation conditions.
- Validate the proposed entropy-based damage approach in corrosion-fatigue against other aluminum alloys and steel materials.
- Validate the proposed entropic-damage theory at different ranges over the corrosion polarization curve [i.e., corrosion dissolution of anodic species (α phase) and corrosion dissolution of cathodic species (β phase)].
- Use various measurement techniques to improve on the measurement of thermodynamic forces and fluxes resulting from other dissipative processes such as heat conduction, diffusion, and hydrogen embrittlement that this study found to have an insignificant contribution to entropy.
- Develop a new approach that accounts for the initial entropic damages such as pit initiation in the pre-corrosion phase, which this study assumed to be zero.
- Develop proof of the independence of entropy generation at the fixed entropic-endurance points for other geometries by performing experiments using more complex geometries.

- Investigate the synergistic effects between thermodynamic fluxes and forces when multiple dissipative processes are active during corrosion-fatigue degradation mechanisms.
- Perform corrosion-fatigue tests in different environmental conditions (e.g., different corrosive solution concentration and pH, different temperature and pressure).
- Develop similar entropic-damage models for other critical failure mechanisms such as stress-corrosion-cracking, radiation embrittlement, and creep failure mechanisms.
- Characterization of the proposed entropy-damage theory in the context of statistical mechanics. This brings about the probabilistic interpretation of damage, based on the probability of the underlying microstructural states.
- Examin the proposed entropic-based-damage approach along with reliability and PHM entropy based techniques through the use of data resulted from other failure mechanisms.

9. References

[1] K. Sieradzki, "Atomistic & Microchemical Aspects of Environment Induced Cracking of Metals," in *Gangloff, R.P., Ives, M.B. (Eds.), First International Conference on Environment-Induced Cracking of Metals, NACE*, Houston, TX, 1990.

[2] D. Kondepudi and I. Prigogine, Modern Thermodynamics: From Heat Engines to Dissipative Structures, England: Jhon Wiley & Sons, 1998.

[3] Military Handbook for Reliability Prediction of Electronic Equipment, Version A, U. S.: Department of Defense, 1965.

[4] "Reliability Prediction Procedure for Electronic Equipment, Telcordia Technologies. Special Report SR-332," Telcordia Customer Service, Piscataway, NJ, 2001.

[5] "Reliability Methodology for Electronic Systems, FIDES Guide Issue," FIDES Group, 2004.

[6] IEEE Standard 1413, "IEEE Standard Methodology for Reliability Prediction and Assessment for Electronic Systems and Equipment," 1998.

[7] IEEE Standard 1413.1, "IEEE Guide for Selecting and Using Reliability Predictions Based on IEEE 1413," 2002.

[8] S. S. Manson, Thermal Stress and Low Cycle Fatigue, New York: McGraw-Hill, 1996.

[9] K. Norris and A. Landzberg, "Reliability of Controlled Collapse Interconnections," *IBM Journal of Research and Development,* vol. 13, pp. 266-277, 1969.

[10] R. Bayerer, T. Hermann, T. Licht, J. Lutz and M. Feller, "Model for Power Cycling Lifetime of IGBT Modules - Various Factors Influencing Lifetime," in *Integerated Power Electronics Systems Conference*, Nuremberg, Germany, 2008.

[11] R. Shi and S. Mahadevan, "Damage Tolerance Approach for Probabilistic Pitting Corrosion Fatigue Life Prediction," *Journal of Engineering Fracture Mechanics,* vol. 68, pp. 1493-1507, 2001.

[12] D. G. Harlow and R. P. Wei, "A Probability Model for the Growth of Corrosion Pits in Aluminum Alloys Induced by Constituent Particles," *Journal of Engineering Fracture Mechanics,* vol. 59, pp. 305-325, 1998.

[13] M. Modarres, M. Kaminskiy and V. Krivtsov, Reliability Engineering and Risk Analysis A Practical Guide, Boca Raton, FL, USA: Taylor and Francis Group, 2010.

[14] J. F. Archard, "Contact and Rubbing of Flat Surfaces," *Appied Physics*, vol. 24, pp. 981-988, 1953.

[15] G. R. Manson. S. S. and Halford, "Practical Implementation of the Double Linear Damage Rule and Damage Curve Approach for Treating Cumulative Fatigue Damage," *International Journd of Fatigue*, vol. 17, no. 2, pp. 169-192, 1981.

[16] M. A. Miner, "Cumulative Damage in Fatigue," *Journal of Applied Mechanics*, vol. 67, pp. 159-164, 1945.

[17] I. R. Kramer, "A Mechanism of Fatigue Failure," *Metallurgical Transactions*, vol. 5, pp. 1737-1742, 1974.

[18] Z. Azari, M. Lebienvenu and G. Pluvinage, "Functions of Damage in Low-cycle Fatigue," *In Advances in Fracture Research*, vol. 3, pp. 1815-1821, 1984.

[19] I. Cordero, A. Ahmadieh and P. K. Mazumdar, "A Cumulative Fatigue Damage Formulation for Persistent Slip Band Type," *Scripta Metallurgica*, vol. 22, pp. 1761-1764, 1988.

[20] F. E. Richart and N. M. Newmark, "A Hypothesis for the Determination of Cumulative Damage in Fatigue," *American Society for Testing and Materials*, vol. 48, pp. 767-800, 1948.

[21] R. R. Gatts, "Application of a Cumulative Damage Concept to Fatigue," *ASME Journal of Basic Engineering*, vol. 83, pp. 529-540, 1961.

[22] J. Lemaitre, A Course on Damage Mechanics, France: Springer, 1996.

[23] R. E, Friction and Wear of Materials, New York: Wiley, 1965.

[24] N. P. Suh, "The Delamination Theory of Wear," *Wear*, vol. 25, pp. 111-124, 1973.

[25] H. K. Birnbaum, "Mechanisms of Hydrogen Related Fracture of Metals in Environment Induced Cracking of Metals," in *Gangloff, R.P., Ives, M.B. (Eds.), First International Conference on Environment-Induced Cracking of Metals; NACE*, Houston, TX, 1990.

[26] D. Duquette, "Corrosion Fatigue Crack Initiation Processes: A State of the Art Review," in *Gangloff, R.P., Ives, M.B. (Eds.), First International Conference on Environment-Induced Cracking of Metals; NACE*, Houston, Texas, 1990.

[27] M. Amiri and M. Modarres, "An Entropy-Based Damage Characterization," *Journal of Entropy*, vol. 16, pp. 6434-6463, 2014.

[28] J. Weertman and J. Weertman, Elementary Dislocation Theory, NY: Oxford University Press: New York, 1992.

[29] E. Gutman, Mechanochemistry of Materials, Cambridge: Cambridge International Science Publishing, 1998.

[30] B. Lu and J. Luo, "Synergism of Electrochemical and Mechanical Factors in Erosion-Corrosion," *Journal of Physics Chemistry*, vol. 110, pp. 4217-4231, 2006.

[31] H. Uhlig and R. Revie, Corrosion and Corrosion Control, 3rd ed., NY: Wiley: New York, 1985.

[32] S. Li and C. A. Basaran, "Computational Damage Mechanics Model for Thermomigration," *Journal of Mechanics of Materials,* vol. 41, pp. 271-278, 2009.

[33] M. Nosonovsky and B. Bhushan, "Thermodynamics of Surface Degradation, Self-Organization, and Self-Healing for Biomimetic Surfaces.," *Philos. Trans,* vol. 367, pp. 1607-1627, 2009.

[34] H. Abdel-Aal, "On the Role of Intrinsic Material Response in Failure of Tribo Systems," *Journal of Wear,* vol. 259, pp. 1372-1381, 2005.

[35] I. Boltzmann, Lectures on Gas Theory, California: University of California Press, Berkeley, 1898.

[36] D. Halliday and R. Resnick, Physics, New York: John Wiley & Son, 1966.

[37] C. Basaran and C. Y. Yan, "A Thermodynamic Framework for Damage Mechanics of Solder Joints," *Journal of Electronic Packaging Transaction of ASME,* vol. 120, pp. 379-384, 1998.

[38] C. Basaran and H. Tang, "Implementation of a Thermodynamic Framework for Damage Mechanics of Solder Interconnects in Microelectronics Packaging," *International Journal of Damage Mechanics,* vol. 11, pp. 87 - 108, 2002.

[39] C. Basaran and S. Nie, "A Thermodynamics Based Damage Mechanics Model for Particulate Composites," *International Journal of Solids and Structures,* vol. 44, no. 3, pp. 1099 - 1114, 2007.

[40] C. Basaran and S. Nie, "An Irreversible Thermodynamic Theory for Damage Mechanics of Solids," *International Journal of Damage Mechanics,* vol. 13, no. 3, pp. 205 - 224, 2004.

[41] T. Temfack and C. Basaran, "Experimental Verification of Thermodynamic Fatigue Life Prediction Model Using Entropy as Damage Metric," *Materials Science and Technology,* vol. 31, no. 13, pp. 1627-1632, 2015.

[42] J. P. Tucker, D. D. K. Chan, G. G. Subbarayan and C. A. Handwerker, "Maximum Entropy Fracture Model and Fatigue Fracture of Mixed SnPb/Sn3.0Ag0.5Cu Solder Alloys," in *13th IEEE Intersociety Conference on Thermal and Thermomechanical Phenomena in Electronic Systems*, San Diego, CA, USA, 2012.

[43] D. Chan, G. Subbarrayan and L. Nguyen, "Maximum-Entropy Principle for Modeling Damage and Fracture in Solder Joints," vol. 41, no. 2, 2012.

[44] R. Bowley and M. Sanchez, Introductory Statistical Mechanics, 2nd edition, Oxford: Oxford University Press, 1999.

[45] G. Lebon, D. Jou and J. Casas-Vázquez, Understanding Non-equilibrium Thermodynamics, Berlin: Springer, 2008.

[46] A. A. Feinberg and A. Widom, "On Thermodynamic Reliability Engineering," *IEEE Transaction on Reliability,* vol. 49, p. 136–146, 2000.

[47] A. A. Feinberg and A. Widom, "Connecting Parametric Aging to Catastrophic Failure Through Thermodynamics," *IEEE Transaction on Reliability,* vol. 45, p. 28–33, 1996.

[48] M. Amiri and M. Khonsari, "On the Thermodynamics of Friction and Wear—A Review," *Journal of Entropy,* pp. 1021-1049, 2010.

[49] B. E. Klamecki, "An Entropy Based Model of Plastic Deformation Energy Dissipation in Sliding," *Journal of Wear,* vol. 96, pp. 319-329, 1984.

[50] K. l. Doelling, F. F. Ling, M. D. Bryant and B. P. Heilman, "An Experimental Study of the Correlation between Wear and Entropy Flow in Machinery Components," *Journal of Applied Physics,* vol. 88, pp. 2999-3003, 2000.

[51] D. Maugis, Contact, Adhesion, and Rupture of Elastic Solids;, Berlin: Springer:, 2000.

[52] V. L. Ontiveros, "Strain Energy and Thermodynamic Entropy as Prognastic Measure of Crack Initiation in Aluminum," PhD Dissertation, Uiversity of Maryland, Maryland, USA, 2013.

[53] H. Tang and C. Basaran, "A Damage Mechanics Based Fatigue Life Prediction Model," *Trans. of ASME, Journal of Electronic Packaging,* vol. 125, pp. 120-125, 2003.

[54] P. W. Whaley, P. Chen and G. M. Smith, "Continuous Measurement of Material Damping during Fatigue Tests," *Journal of Experimental Mechanics,* vol. 24, pp. 342-348.

[55] P. W. Whaley, Y. Pao and K. Lin, "Numerical Simulation of Material Fatigue by a Thermodynamic Approach," in *24th Structural Dynamic and Material Conference*, Lake Tahoe, Nevada, 1983.

[56] P. W. Whaley, "A Thermodynamic Approach to Metal Fatigue," in *ASME International Conference on Advances in Life Prediction Methods*, Allbany, 1983.

[57] Y. F. Ital'yantsev, "Thermodynamic State of Deformed Solids. Report 1. Determination of Local Function of State," *Strength Material,* vol. 16, pp. 238 - 241, 1984.

[58] Y. F. Ital'yantsev, "Thermodynamic State of Deformed Solids. Report 2. Entropy Failure Criteria and Their Application for Simple Tensile Loading Problems," *Strength Material,* vol. 16, pp. 242-247, 1984.

[59] M. Naderi, M. Amiri and M. Khonsari, "On the Thermodynamic Entropy of Fatigue Fracture," *Processing of Royal Socity,* vol. 466, pp. 423-438, 2010.

[60] M. Amiri and M. M. Khonsari, "On the Role of Entropy Generation in Processes Involving Fatigue," *Entropy,* vol. 14, pp. 24 - 31, 2012.

[61] F. F. Ling, M. D. Bryant and K. L. Doelling, "On Irreversible Thermodynamics for Wear Prediction," *Wear* , vol. 253, pp. 1165-1172, 2002.

[62] M. Bryant, "Unification of Friction and Wear," in *in: Nikas, G. (Ed.): Recent Developments in Wear Prevention, Friction, and Lubrication*, Kerala, 2010.

[63] Z. Y. S. Dai and Q. Xue, "Thermodynamic Model of Fretting Wear," *Journal of Nanjing University Aeronautics and Astronautics,* vol. 32, pp. 125 - 131, 2000.

[64] M. Smetanin, Q. Denga and J. R. Weissmu, "Dynamic Electro-Chemo-Mechanical Analysis During Cyclic Voltammetry," *Journal of Physics Chemistry,* vol. 13, pp. 17313-17322, 2011.

[65] G. Valincius, "Electrocapillary Equations of Solid Electrodes," *Journal of Electroanalytical Chemistry,* vol. 478, p. 40, 1999.

[66] M. Sahal, J. Creus, R. Sabot and X. Feaugas, "The Effects of Dislocation Patterns on the Dissolution Process of Polycrystalline Nickel," *Journal of Acta Materialia* , vol. 54, p. 2157–2167, 2006.

[67] M. Ieong, B. Doris, J. Kedzierski, K. Rim and M. Yang, "Silicon Device Scaling to the Sub-10-nm Regime," *Journal of Science,* vol. 306, pp. 2057-2060, 2004.

[68] Y. S. Choi, T. Numata, T. Nishida, R. Harris and S. E. Thompson, "Impact of Mechanical Stress on Gate Tunneling Currents of Germanium Silicon P-Type Metal-Oxide-Semiconductor Field-Effect Transistors and Metal Gate Work Function," *Journal of Applied Physics,* vol. 103, 2008.

[69] F. Larché and J. W. Cahn, "The Effect of Self-Stress on Diffusion in Solids," *Journal of Acta Metallica,* vol. 30, pp. 1835-1845, 1982.

[70] F. C. Larché and J. W. Cahn, "The Interactions of Composition and Stress in Crystalline Solids," *Journal of Acta Metallica,* vol. 33, pp. 331-357, 1985.

[71] M. H. Stashchuk, "Anodic Regions on The Boundary between an Elliptic Hole and a Medium," *Journal of Materials Science, Vol. 46, No. 4, January, 2011,* vol. 46, no. 4, pp. 36-54, 2011.

[72] L. Onsager, "Reciprocal Relations in Irreversible Processes," *Journal of Physics,* vol. 37, pp. 2265-2279, 1931.

[73] S. X. Mao and M. Li, "Mechanics and Thermodynamics on the Stress and Hydrogen Interaction in Crack Tip Stress Corrosion: Experiment and Theory," *Journal of Mechanics Physics and Solids,* vol. 46, pp. 1125-1137, 1998.

[74] L. J. Qiao and S. X. Mao, "Thermodynamic Analysis on the Role Of Hydrogen in Anodic Stress Corrosion Cracking," *Journal of Acta Metal Materials,* vol. 43, pp. 3989 - 4001, 1995.

[75] M. Mavrikakis, B. Hammer and J. K. Nørskov, "Effect of Strain on the Reactivity of Metal Surfaces," *Journal of Physics,* vol. 81, pp. 19 - 28, 1998.

[76] A. Horva´ and R. Schiller, "The Effect of Mechanical Stress on the Potential of the Ag/Ag+ Electrod," *Journal of Physics,* vol. 3, pp. 26 - 62, 2001.

[77] M. Smetanin, "Mechanics of Electrified Interfaces in Diluted Electrolytes," PhD dissertation, 2010.

[78] M. Bryant, M. Khonsari and F. Ling, "On the Thermodynamics of Degradation," *Processing of Rpyal Society,* vol. 464, pp. 2001-2014, 2008.

[79] C. Cheng and M. Pecht, "A Fusion Prognostics Method for Remaining Useful Life Prediction of Electronic Products," in *5th annual IEEE Conference on Automation Science and Engineering*, Bangalore, India, 2009.

[80] J. Lu and W. Meeker, "Using Degradation Measures to Eestimate a Time-to-failure Distribution," *Technometrics,* vol. 35, no. 2, pp. 161-173, 1993.

[81] M. Rausand and A. Høyland, System Reliability Theory Models, Statistical Methods, and Applications, New Jersey: Wiley & Sons, 2004.

[82] C. Byington, M. Watson and D. Edwards, "Data-Driven Neural Network Methodology to Remaining Life Predictions for Aircraft Actuator Components," in *Proceedings of the IEEE Aerospace Conference*, New York, USA, 2004.

[83] M. Schwabacher and K. Goebel, "A Survey of Artificial Intelligence for Prognostics," in *AAAI Fall Symposium: AI for Prognastics*, 2007.

[84] B. S. Bhangu, P. Bentley, D. A. Stone and C. M. Bingham, "Nonlinear Observers for Predicting State-of-Charge and State-of-Health of Lead-Acid Batteries for Hybrid-Electric Vehicles," *IEEE Transactions on Vehicular Technology,* vol. 54, no. 3, pp. 783-798, 2005.

[85] M. S. Arulampalam, S. Maskell, N. Gordon and T. Clapp, "A Tutorial on Particle Filters for Online Nonlinear/Non-Gaussian Bayesian Tracking," *IEEE Transaction on Signal Processing*, vol. 50, no. 2, pp. 174-189, 2002.

[86] M. Orchard, B. Wu and G. Vachtsevanos, "A Particle Filtering Framework for Failure Prognosis," in *Proceedings of the World Tribology Congress*, 2005.

[87] S. Kumar, M. Torres, Y. Chan and M. Pecht, "A hybrid prognostics methodology for electronic products," in *IEEE World Congress on Computational Intelligence*, Hong Kong, 2008.

[88] B. H. Nystad, "Technical Condition Indexes and Remaining Useful Life of Aggregated Systems," Doctoral dissertation. Norwegian University of Science and Technology (NTNU), Trondheim, Norway, 2008.

[89] H. S. Leff, "Removing the Mystery of Entropy and Thermodynamics – Part V," *The Physics Teacher,* vol. 50, pp. 274-276, 2012.

[90] T. B. Mills, D. J. Magda, S. E. Kinyon and D. W. Hoeppner, "Fatigue crack," Report to Oklahoma City Air Logistics Center and Boeing Defense and Space, 1995.

[91] D. W. Hoeppner, "Parameters that Input to Application of Damage Tolerance Concepts to Critical Engine Components," in *AGARD Conference*, San Antonio, Texas, USA, 1985.

[92] C. A. Arriscorreta, "Statistical Modeling for the Corrosion Fatigue of Aluminum Alloys 7075-T6 And 2024-T3," PhD Dissertation, Utah, 2012.

[93] Y. Kondo, "Prediction of Fatigue Crack Initiation Life Based on Pit Growth," *Journal of Corrosion Science,* vol. 45, pp. 7 - 11, 1989.

[94] T. C. Lindley, P. McIntyre and P. J. Trant, "Fatigue Crack Initiation at Corrosion Pits," *Journal of Metals Technology,* vol. 9, pp. 135 - 142, 1982.

[95] D. W. Hoeppner, "Model for Prediction of Fatigue Lives Based Upon a Pitting Corrosion Fatigue Process," *Journal of American Society for Testing and Materials (ASTM),* pp. 841 - 870, 1979.

[96] J. D. Atkinson, J. Yu, Z. Y. Chen and Z. J. Zhao, "Modeling of Corrosion Fatigue Crack Growth Plateux for RPV Steels in High Temperature Water," *Journal of Nuclear Engineering and Design,* vol. 184, pp. 13-25, 1998.

[97] D. W. Hoeppner, V. Chandrasekaran and A. Taylor, "Review of Pitting Corrosion Fatigue Model," in *20th ICAF Symposium, Structural Integrity for the Next Millenium*, Dayton, OH, USA, 2000.

[98] W. Rong, "A Fracture Model of Corrosion Fatigue Crack Propagation of Aluminum Alloys Based on the Material Elements Fracture Ahead of a Crack Tip," *International Journal of Fatigue,* vol. 30, pp. 1376-1386, 2008.

[99] J. Noortwijk and M. Van, "A Survey of the Application of Gamma Processes in Maintenance," *Reliability Engineering and System Safety,* vol. 94, pp. 2-21, 2009.

[100] K. Sankaran, R. P. a and K. Jata, "Effects of Pitting Corrosion on the Fatigue Behavior of Aluminum Alloy 7075-T6: Modeling and Experimental Studies," *Journal of Materials Science and Engineering,* vol. 297, pp. 223-229, 2001.

[101] J. W. Gibbs, The Scientific Papers of J. Williard Gibbs, vol. 1, Thermodynamics, Woodbridge: Ox Bow Press, 1993.

[102] H. Ziegler, An Introduction to Thermomechanics, North-Holland, Amesterdam, 1983.

[103] S. R. De Groot and P. Mazur, Non-Equilibrium Thermodynamics, New York: John Wiley & Sons, 1962.

[104] P. W. Bridgman, The Nature of Thermodynamics, Cambridge: Harvard University Press, 1941.

[105] E. Jaynes, "Information Theory and Statistical Mechanics," *Physical Review,* vol. 106, no. 4, pp. 620 - 630, 1957.

[106] C. E. Shannon, "A Mathematical Theory of Communication," *Journal of Bell System Technology,* vol. 27, pp. 379-423, 1948.

[107] M. Roemer, J. Ge, A. Liberson, G. Tandon and R. Kim, "Autonomous Impact Damage Detection and Isolation Prediction for Aerospace Structures," in *Proceeding of the IEEE Aerospace Conference*, New York, USA, 2005.

[108] L. Studer and F. Masulli, "On The Structure Of A Neuro-Fuzzy System to Forecast Chaotic Time Series," in *Proceedings of the International Symposium on Neuro-Fuzzy Systems*, 1996.

[109] J. Sheldon, H. Lee, M. Watson, C. Byington and E. Carney, "Detection of Incipient Bearing Faults in a Gas Turbine Engine Using Integrated Signal Processing Techniques," in *Proceedings of the American Helicopter Society Annual Forum,*, Alexandria, VA: AHS, 2007.

[110] F. He and W. Shi, "WPT-SVMs Based Approach for Fault Detection of Valves in Reciprocating Pumps," in *American Control Conference*, 2002.

[111] M. E. Tipping, "The Relevance Vector Machine," *Journal of Advances in Neural Information Processing Systems,* vol. 12, pp. 652-658, 2000.

[112] V. N. Vapnik, The Nature of Statistical Learning, Berlin: Springer, 1995.

[113] C. Stander and P. Heyns, "Instantaneous Angular Speed Monitoring of Gearboxes under Non–cyclic Stationary Load Conditions," *Journal of Mechanical Systems and Signal Processing,* vol. 19, no. 4, pp. 817-835, 2005.

[114] W. Bartelmus and R. Zimroz, "A New Feature for Monitoring the Condition of Gearboxes in Non–stationary Operating Conditions," *Journal of Mechanical Systems and Signal Processing,* vol. 23, no. 12, pp. 1528-1534, 2009.

[115] S. Amin, C. Byington and M. Watson, "Fuzzy Inference and Fusion for Health State Diagnosis of Hydraulic Pumps and Motors," in *Proceeding of the Annual Meeting of the North American Fuzzy Information Processing Society*, Detroit, MI, 2005.

[116] D. Brown, P. Kalgren, M. Roemer and T. Dabney, "Electronic Prognostics – A Case Study Using Switched-Mode Power Supplies (SMPS)," in *IEEE Systems Readiness Conference*, New York, 2006.

[117] M. Byington and C. Roemer, "Prognostics and Health Management Software for Gas Turbine Engine Bearings," in *Proceedings of the ASME Turbo Exposition*, New York, 2007.

[118] S. Kumar and M. Pecht, "Health Monitoring of Electronic Products Using Symbolic Time Series Analysis," in *Artificial Intelligence for Prognostics, AAAI Fall Symposium Series*, Arlington, VA, 2007.

[119] B. Saha, K. Goebel, S. Poll and J. Christopherson, "An Integrated Approach to Battery Health Monitoring using Bayesian Regression, Classification and State Estimation," in *IEEE Conference*, New York, 2007.

[120] J. M. Noortwijk, "A Survey of the Application of Gamma Processes in Maintenance," *Reliability Engineering and System Safety*, vol. 94, pp. 2-21, 2009.

[121] R. P. Gangloff, "Corrosion Fatigue Cracking, in Corrosion Tests and Standards: Application and Interpretation," in *Journal of American Society for Testing and Materials (ASTM)*, 2005.

[122] D. A. Jones, Principles and Prevention of Corrosion, 2nd ed., NJ: Upper Hall, Upper Saddle River, 1996.

[123] M. S. Seller, A. J. Schultz, C. Basaran and D. A. Kofke, "bSn Grain Boundary Structure and Self-diffusivity via Molecular Dynamics Simulation," *Journal of Physics Review B. 134111,* 2010.

[124] H. Kamoutsi, G. Haidemenopoulos, V. Bontozoglou and S. Pantelakis, "Corrosion-induced Hydrogen Embrittlement in Aluminum Alloy 2024," *Corrosion Science,* vol. 48, no. 5, pp. 1209-1224, 2006.

[125] N. Takano, "Hydrogen Diffusion and Embrittlement in 7075 Aluminum Alloy," in *14th International Conference on the Strength of Materials*, 2008.

[126] A. S. El-Amoush, "An Investigation of Hydrogen-induced Hardening in 7075-T6 Aluminum Alloy," *Journal of Alloys and Compounds,* vol. 465, no. 1, pp. 497-501, 2008.

[127] B. Gu, J. Luo and X. Mao, "Hydrogen-Facilitated Anodic Dissolution-Type Stress Corrosion Cracking of Pipeline Steels in Near-Neutral pH Solution," *Corrosion,* vol. 55, no. 1, pp. 96-106, 1999.

[128] B. T. Lu, J. Luo, P. Norton and H. Ma, "Effects of Dissolved Hydrogen and Elastic and Plastic Deformation on Active Dissolution of Pipeline Steel in Anaerobic Groundwater of Near-Neutral pH," *Acta Materials,* vol. 57, pp. 41 - 49, 2009.

[129] L. J. Qiao, J. L. Luo and X. Mao, "The Role of Hydrogen in the Process of Stress Corrosion Cracking of Pipeline Steels in Dilute Carbonate-Bicarbonate Solution," *Journal of Materials Science Letters,* vol. 16, no. 7, pp. 516- 520, 1997.

[130] X. Hu, Z. Huang, L. Qiao and W. Chu, "Effect of Hydrogen and Stress on Anodic Dissolution," *Journal of Chinese Society for Corrosion and Protection,* vol. 16, p. 187, 1996.

[131] T. S. Sudarshan and M. R. Louthan, "Gaseous Environment Effect on Fatigue Behaviour of Metals," *International Materials Reviews,* vol. 32, no. 3, pp. 121-151, 1987.

[132] N. Grinberg, "The Effect of Vacuum on Fatigue Crack Growth," *International Journal of Fatigue,* vol. 4, no. 2, pp. 83-95, 1982.

[133] L. Jing-jing, S. Jun-jun and H. Hai-yun, "The Life Prediction for Materials under the Corrosion of Seawater," *Acta Physica Sinica,* vol. 54, no. 5, pp. 2414-2417, 2005.

[134] X. g. Huang, J. Q. Xu and M. L. Feng, "Energy Principle of Corrosion Environment Accelerating Crack Propagation during Anodic Dissolution Corrosion Fatigue," *Journal of Shanghai Jiaotong University,* vol. 18, no. 2, pp. 190-196, 2013.

[135] A. A. Griffith, "The Phenomena of Rupture and Flow in Solids," *Transaction of Royal Society*, vol. 221, pp. 163-198, 1921.

[136] H. Xiao-guang, X. Jin-quan and F. Miao-lin, "Energy Principle of Corrosion Environment Accelerating Crack Propagation During Anodic Dissolution Corrosion Fatigue," *Journal of Shanghai Jiaotong Univ. (Sci.), 2013,* vol. 18, no. 2, pp. 190-196, 2013.

[137] Y. G. Chun and S. I. Pyun, "Crack Closure in the Fatigue Crack Propagation of a Cu-2wt.%Be Alloy in Dry Air and Ammoniacal Solution," *Material Science and Engineering*, vol. 206, no. 1, pp. 49-54, 1996.

[138] O. R. Romaniv, G. N. Nikiforchin and N. N. Andrusiv, "The Effect of Cracks Closure and the Estimation of Cyclic Crack Resistance of Structural Alloys," *Journal of Physico- Chemistry, Mechanics & Materials*, vol. 3, pp. 47-61, 1983.

[139] M. D. Fontea, F. Romeirob and M. D. Freitasc, "The Effect of Microstructure and Environment on Fatigue Crack Propagation in 7049 Aluminium Alloy at Negative Stress Ratios," *International Journal of Fatigue,* vol. 25, no. 9, pp. 1209-1216, 2003.

[140] R. P. Gangloff, "Crack Size Effects on the Chemical Driving Force for Aqueous Corrosion Fatigue," *Metallurigical and Materials Transaction,* vol. 16, no. 5, pp. 953-969, 1985.

[141] H. A. Bruck, S. R. McNeill, M. A. Sutton and W. H. P. Iii, "Digital Image Correlation Using Newton-Raphson Method of Partial Differential Correction," *Experimental Mechanics,* vol. 29, no. 3, pp. 261-267, 1989.

[142] N. D. Alexopoulos and P. Papanikos, "Experimental and Theoretical Studies of Corrosion-Induced Mechanical Properties Degradation of Aircraft 2024 Aluminum Alloy," *Journal of Material Science and Engineering,* vol. 498, pp. 248-257, 2008.

[143] J. Xiao and S. Chaudhuri, "Predictive Modeling of Localized Corrosion: An Application to Aluminum Alloys," *Journal of Electrochimica Acta,* vol. 56, pp. 5630-5641, 2011.

[144] N. Birbilis and R. G. Buchheit, "Electrochemical Characteristics of Intermetallic Phases in Aluminum Alloys An Experimental Survey and Discussion," *Journal of The Electrochemical Society,* vol. 152, no. 4, pp. 140-151, 2005.

[145] P. Pao, C. Feng and S. Gill, " Corrosion Fatigue Crack Initiation in Aluminum Alloys 7075 and 7050," *Journal of Corrosion,* vol. 10, pp. 1022-1032, 2000.

[146] O. Guseva, P. Schmutz, T. Suter and O. Trzebiatowski, "Modelling of Anodic Dissolution of Pure Aluminium in Sodium Chloride," *Journal of Electrochemical Acta,* vol. 54, pp. 5414-5424, 2009.

[147] T. H. Nguyen and R. Foley, "The Chemical Nature of Aluminum Corrosion II the Initial Dissolution Step," *Journal of Electrochemical Society,* vol. 129, pp. 27 - 32, 1982.

[148] H. d. Costa-Matto and P. Pacheco, "Non-Isothermal Low-Cycle Fatigue Analysis of Elasto-Viscoplastic Materials," *Mechanics Research Communications,* vol. 36, no. 4, pp. 428-436, 2009.

[149] N. S. Altman, "An Introduction to Kernel and Nearest-Neighbor Nonparametric Regression," *The American Statistician,* vol. 46, no. 3, pp. 175 - 185, 1992.

[150] M. Abdel-Hameed, "A Gamma Wear Process. IEEE," *Transactions on Reliability, 24(2), 152-153,* vol. 24, no. 2, pp. 152-153, 1975.

[151] P. F. Fantoni and A. Nordlund, "Wire System Aging Assessment and Condition Monitoring," *NKS-130. ISBN 87-7893-192-4,* 2009.

[152] M. Liakat and M. Khonsari, "An Experimental Approach to Estimate Damage and Remaining Life of Metals under Uniaxial Fatigue Loading," *Journal of Material & Design,* vol. 57, pp. 289-297, 2014.

[153] S. R. de Groot and P. Mazur, Non-Equilibrium Thermodynamics, New York: John Wiley & Sons, 1962.